

Concept of risk-aware contrail avoidance strategies

Audran Borella^{1,*}, Cameron Steer¹, Nicolas Bellouin^{1,2}, and Olivier Boucher¹

¹Institut Pierre-Simon Laplace, Sorbonne Université / CNRS, Paris, France

²Department of Meteorology, University of Reading, Reading, UK

* now at: Klima Consulting, Paris, France

Correspondence: Audran Borella (audran.borella@klima-consulting.fr)

Abstract. Targeted contrail avoidance consists of rerouting aircraft to minimise the formation of contrails whose warming of the climate system can be much larger than that due to the CO₂ emitted for some of the flights. A commonly proposed strategy is to reroute all flights for which the trade-off between additional CO₂ emissions and reduction in contrail warming leads to a climate benefit. However, current predictions of contrail climate impact are highly uncertain. In this study, we describe 5 a framework to integrate the risk of unintentionally damaging the climate in the contrail avoidance decision-making process, using the Contrail Cirrus Prediction model (CoCiP) and operational ensemble weather forecasts. Optimising trajectories around a best estimate of contrail radiative forcing then including weather and parametric uncertainties in that predicted forcing in a second step reveals that 55% of the reroutings have a higher-than-5% risk of unintentionally damaging the climate compared to a standard risk-unaware avoidance strategy. This fraction increases to 76% when choosing to reject any risk. However, the 10 reroutings that are the least risky to operate are also those with the highest potential climate benefit, often referred to as ‘big hits’. Alternatively, accounting for uncertainties from the start of trajectory optimisation allows to mitigate the risk directly when planning the flight. This strategy would even result in a 52% higher potential climate benefit compared to the risk-unaware avoidance strategy, when choosing to reject any risk. Our results thus demonstrate that the risk of unintentionally damaging the climate can and should be included in the decision-making of contrail avoidance, in particular in the context of 15 early adoption policies.

1 Introduction

Aviation was responsible for about 2.4% of the total anthropogenic CO₂ emissions in 2018 (ICCT, 2018; Klöwer et al., 2021; Jaramillo et al., 2023). However, its climate impact also originates from non-CO₂ effects, such as the formation of condensation trails (contrails), NO_x emissions, or stratospheric H₂O emissions (Brasseur et al., 2016; EASA, 2020). Including such effects, 20 the contribution of aviation to the total anthropogenic effective radiative forcing (ERF), an integrated climate impact indicator, is about 3.5% for the period 1940 to 2018 (Lee et al., 2021). The ERF of non-CO₂ effects from aviation is estimated to be twice that of CO₂, with contrails having the largest contribution. However, it is also associated with a significant uncertainty, with an ERF lying between half and three times that of CO₂. Contrails are formed in the wake of aircraft when specific weather conditions are met (Schumann, 1996) and persist when they are formed in ice supersaturated regions (ISSRs), where saturation 25 with respect to ice exceeds 100% (Gierens et al., 2012). Depending on the properties of the aircraft and fuel, and on the weather

conditions, persistent contrails can evolve into contrail cirrus within a few hours, leading to a substantial warming potential (Burkhardt and Kärcher, 2011; Kärcher, 2018).

Although the efforts to reach CO₂ emissions reduction targets should be prioritised (Lee et al., 2023), reducing the non-CO₂ effects at the cost of slightly increased CO₂ emissions should be beneficial for the climate overall (Prather et al., 2025; Smith 30 et al., 2025; Johansson et al., 2025). Two main strategies have been proposed and tested to reduce the impact of contrails without waiting for technological improvements, namely the reduction of aircraft soot number emissions (Burkhardt et al., 2018; Voigt et al., 2021; Märkl et al., 2024; Quante et al., 2024) and contrail avoidance (Mannstein et al., 2005; Rosenow et al., 2018; Molloy et al., 2022). The latter strategy may consist of strictly avoiding the formation of all persistent contrails, whether they are strongly or slightly warming (Sausen et al., 2024; Sonabend-W et al., 2024), or may focus on avoiding the 35 formation of the most warming contrails, an approach known as targeted contrail avoidance (Grewe et al., 2017; Martín Frías et al., 2024; Simorgh and Soler, 2025). Avoiding the formation of all persistent contrails implies that all flights forming such contrails should be rerouted, representing about 20% of all flights (Teoh et al., 2024a). On the contrary, avoiding only the most warming contrails limits the impact of contrail avoidance onto air traffic management, as only about 2–5% of the flights are responsible for 80% of the forcing of contrails (e.g., Teoh et al., 2024a), drastically reducing the number of flights that need to 40 be rerouted.

Avoiding the formation of contrails comes with an additional financial cost, because flights must be deviated from their cost-optimal route (Niklaß et al., 2019; Matthes et al., 2020; Yamashita et al., 2021). In most cases, this leads to increased fuel consumption and fuel-related emissions such as CO₂ and NO_x. Balancing the corresponding additional warming impact with the avoided warming impact from suppressing the contrail effect requires estimating these effects as accurately as possible 45 (Irvine et al., 2014; Borella et al., 2024). Different models have been developed to predict the forcing of potentially formed contrails (Fritz et al., 2020; Yin et al., 2023; Jafarimoghaddam and Soler, 2025). Amongst them, the Contrail Cirrus Prediction model (CoCiP; Schumann, 2012) has been widely used in different studies investigating contrail impact and contrail avoidance (e.g., Teoh et al., 2024a; Sonabend-W et al., 2024; Martín Frías et al., 2024). It is also the model used for reporting the forcing of 50 formed contrails by aircraft departing from and arriving within the European Union, in the framework of the aviation non-CO₂ Monitoring, Reporting, Verification (MRV) scheme (Niklaß et al., 2024).

Targeted contrail avoidance relies primarily on flight planning as it determines the optimal trajectory that balances operational constraints and costs with contrail formation and climate impact, as described in studies that assessed the potential gain of contrail avoidance (Grewe et al., 2017; Martín Frías et al., 2024; Simorgh and Soler, 2025). These studies include no decision-making on whether a flight should be deviated from its cost-optimal route, instead assuming the proposed climate-optimal trajectory is always flown. However, the prediction of the climate impact of individual contrails is highly uncertain, which may influence the decision-making on a flight-by-flight basis (Teoh et al., 2020; Platt et al., 2024; Engberg et al., 2025). These 55 uncertainty stems from, but is not limited to, the parameters of the CoCiP model (Schumann et al., 2012; Platt et al., 2024), its structural limitations (Akhtar Martínez and Jarrett, 2024; Akhtar Martínez et al., 2025), the meteorological data (Gierens et al., 2020; Wolf et al., 2025), or the climate efficacy of contrails (Bickel et al., 2025). Because of these uncertainties, the predicted climate benefit of avoidance may be over- or underestimated. In some cases, the trade-off between fuel-related emissions 60

and contrail impact that is predicted to be beneficial for the climate could in fact be damaging. Such a risk of unintentionally damaging the climate may affect the decision as to whether a flight should be rerouted to avoid contrails, in particular in the context of a no-regret avoidance policy whereby unintended climate damage is to be avoided such that the risk must be 0%. While the previous targeted contrail avoidance approach minimise the overall climate impact of a fleet, it does not inform on 65 such a risk on a flight-by-flight basis. Simorgh et al. (2024b) did integrate weather uncertainties in their optimisation process such that the uncertainty in their predicted climate impact can be minimised, but it is not clear how their method affects the risk of unintentionally damaging the climate for individual flights.

In this study, we describe a framework to integrate the risks of unintentionally damaging the climate in the rerouting decision-making. The impact of such risk-aware contrail avoidance strategies are assessed against a strategy that does not integrate such 70 risks. The uncertainties used to estimate the risks are only those stemming from the CoCiP parameters and from the weather forecast. The other sources of uncertainty are not included because they are difficult to quantify on a flight-by-flight basis at this stage, but we emphasise that they would have to be addressed before large-scale operational contrail avoidance is to be implemented. In this context, the risk-aware contrail avoidance strategies are described in Section 2, and the datasets and tools that we use in Section 3. Section 4 explains the calculation of the risk of unintentionally damaging the climate using 75 two case studies and how decision-making is affected. Broadening the analysis from a single flight to an ensemble of flights is investigated in Section 5. Section 6 investigates a risk-aware strategy directly integrated within the flight planning process and shows its potential in terms of climate benefit. Finally, Section 7 discusses the results and concludes the study.

2 Description of the risk-aware contrail avoidance strategies

We describe three ways to manage weather and contrail prediction uncertainties in climate optimisation of aircraft routes. The 80 most straightforward contrail avoidance strategy is to consider that the prediction of the climate impact is perfect, estimated from a deterministic weather forecast and the nominal configuration of CoCiP, without considering any uncertainty on these two components (e.g., Martín Frías et al., 2024). The cost climate-optimal route can then be determined, and the aircraft flies this route as long as the climate benefit is positive, which should be ensured by the optimisation process (Fig. 1, risk-unaware strategy). The main interest of this strategy is that its operational implementation is easy, as current flight planning systems 85 operate in a similar way. Moreover, the calculations are very cheap. However, it does not integrate the risk of unintentionally damaging the climate, and we name this strategy the risk-unaware strategy in consequence.

This strategy can be improved without disrupting too significantly operational flight planning processes by including in the workflow one additional step related to the risk of unintentionally damaging the climate (Fig. 1, risk-informed strategy). Rather than providing only one cost climate-optimal route, the cost-optimal route is also calculated. From the estimation of contrail 90 climate impact uncertainties, the risk of unintentionally damaging the climate can be estimated. If this risk is above a given threshold, fixed by the airline policy, the aircraft is not rerouted and flies the cost-optimal route. Else, it flies the new, cost climate-optimal route. This strategy has the advantage of being cheap in terms of computational cost, and mostly of being

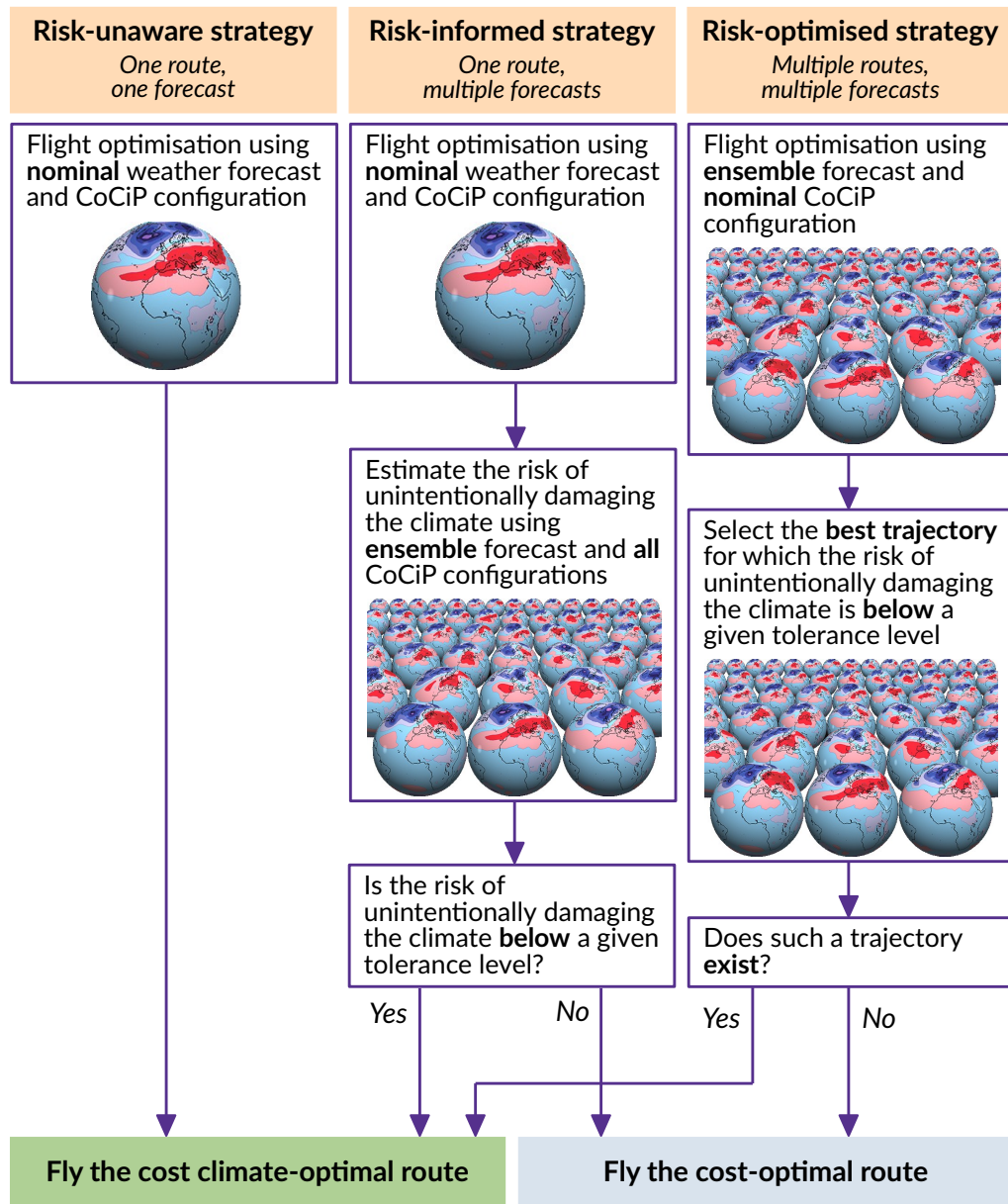


Figure 1. Flowchart of the flight planning process for the three contrail avoidance strategies described. The single forecast pictures indicate nominal estimations with no uncertainties integrated, while the ensemble forecast pictures indicate that uncertainties are taken into account. The pictures are adapted from <https://www.ecmwf.int/en/about/media-centre/focus/2017/fact-sheet-ensemble-weather-forecasting>.



easily adaptable to existing flight planning processes. We name this strategy the risk-informed strategy, corresponding to the first risk-aware strategy described in this study.

95 The proposed cost climate-optimal route in this strategy relies entirely on the nominal CoCiP configuration and on the deterministic weather forecast. However, given the chaotic behaviour of the atmosphere, numerical weather forecasts are often composed of an ensemble-based prediction system, which consists of an ensemble of forecasts generated by perturbing initial conditions. Assuming that all these forecasts are equally probable, and using one or another of the available forecasts as the nominal forecast to optimise the trajectory can lead to very different cost climate-optimal routes. To circumvent this issue, 100 weather uncertainties can be integrated directly into the flight optimisation. Simorgh et al. (2024b) included the uncertainty on the predicted climate impact that stems from the uncertainty in weather prediction directly into the cost function of their optimisation. Here, we propose an alternative method and optimise a given flightpath for all the ensemble members of the weather forecast, providing multiple different trajectories (Fig. 1, risk-optimised strategy). The decision of which route to 105 select out of the different possibilities consists of choosing the route with the highest average climate benefit amongst those for which the risk of unintentionally damaging the climate is below a given threshold. By choosing such a route, we guarantee that the risk is lower than the given threshold while the predicted potential for climate benefit is maximum. While this strategy is the most efficient way of minimising the risk, it requires either substantial modifications to existing flight planning processes, which may take some time, or be time expensive, which is not an option in day-to-day operations. We name this strategy the risk-optimised strategy, corresponding to the second risk-aware strategy described in this study.

110 These contrail avoidance strategies rely on the knowledge of the state of the weather at the time when flight planning occurs. This means that the strategies are based on forecasts available prior to departure, not on reanalysed meteorological data that incorporate later observations. In the following, the two risk-aware strategies are investigated to understand how integrating the risk of unintentionally damaging the climate during contrail avoidance can affect its benefits, compared to the risk-unaware strategy.

115 3 Datasets and tools

3.1 Flight data

We consider in this study the flights that connect the busiest airports of Western Europe (EGLL, EHAM, EDDF, and LFPG), with those of Eastern North America (KJFK, KEWR, and KORD), as depicted in Fig. 2 (see also Table 1 for a description of the airports). We only consider transatlantic flights because the traffic is much less congested and constrained above the North 120 Atlantic Ocean than over Europe or North America, while being still very high. Moreover, contrails are more likely to form and persist above the North Atlantic Ocean than other neighbouring regions (Teoh et al., 2024a). We select only the flights that took off on the 5th, the 15th, and the 25th of March 2024, June 2024, September 2024, and December 2024, in order to reduce computational cost. The days were chosen at random in order to sample each season equally and to account for the different potential formation and evolution mechanisms of contrails that depend on the weather pattern (Teoh et al., 2022).

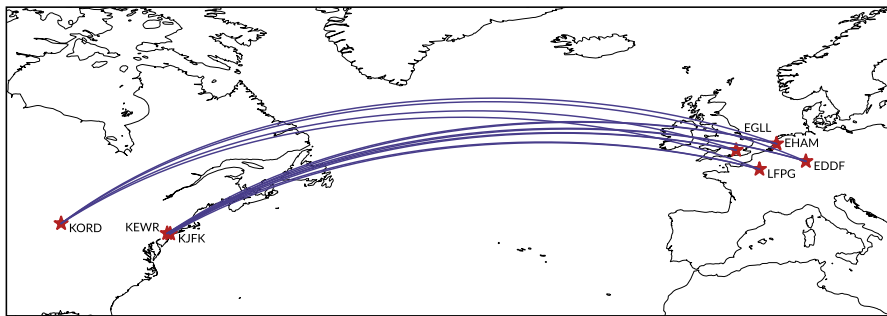


Figure 2. Location of the airports considered in the study. The shortest routes connecting the airports for transatlantic flights are shown. Basemap plotted using Cartopy 0.22.0 and sourced from Natural Earth.

Table 1. List of the airports considered in this study.

ICAO code	Airport name	City, country
EGLL	Heathrow Airport	London, UK
EHAM	Schiphol Airport	Amsterdam, the Netherlands
EDDF	Frankfurt Airport	Frankfurt, Germany
LFPG	Charles-de-Gaulle Airport	Paris, France
KJFK	John-F.-Kennedy Airport	New York, USA
KEWR	Liberty Airport	Newark, USA
KORD	O'Hare Airport	Chicago, USA

125 The data for this subset of flights was retrieved from the FlightRadar24 database (FlightRadar24, 2022). It consists of a pair of departure and arrival airports and times, which allows for the screening described above, as well as the ICAO code of the aircraft type. In total, the subset is composed of 1747 flights, divided into 886 westbound flights and 861 eastbound flights. Amongst these flights, 389 took off in March, 487 in June, 482 in September, and 389 in December.

3.2 Weather forecasts

130 Most studies that investigated operational flight planning including climate costs used reanalysed meteorological data (e.g., Simorgh et al., 2023, 2024b; Martín Frías et al., 2024), such as the ERA5 reanalysis product (Soci et al., 2024). These products are constructed using observations of the atmosphere both before and after the time of a given reanalysis. In operational conditions, observations made after the current time are not available, and flight planners only have access to weather forecasts. To simulate near-operational conditions, we use weather forecasts from the operational archive of the Integrated Forecasting 135 System (IFS) of the European Centre for Medium-Range Weather Forecasts (ECMWF). The IFS developed by the ECMWF is a state-of-the-art numerical weather prediction model used for global weather forecasting (ECMWF, 2024b) recognised by



the scientific community as one of the best in the world. The forecasts are provided with a native resolution of $0.1^\circ \times 0.1^\circ$ on the horizontal and 137 model levels, but we use a resolution degraded to $0.25^\circ \times 0.25^\circ$ and 37 levels interpolated on regular pressure levels to reduce memory usage. At cruise altitudes, the available pressure levels are 150, 200, 250, 300, and 400 hPa, 140 corresponding respectively to about 13.6, 11.8, 10.4, 9.2, and 7.2 km, or 44600, 38700, 34000, 30100, and 23600 feet. For a given flight, the forecast used is the latest one available before departure time, that started at 00 or 12 UTC. The forecast lead time, corresponding to the time between the initial conditions of the forecast and departure, therefore varies between 0 and 12 hours. In fully operational conditions, the lead time would be higher, as a forecast is released a few hours after the time of the initial conditions. Previous studies showed that the higher the lead time, the less likely ISSRs are correctly predicted (von 145 Bonhorst et al., 2025), with the ISSR location often being shifted in space or time rather than being absent (Dean et al., 2025). We leave the analysis of the dependence of contrail avoidance strategies on forecast lead time for future work.

The deterministic (or control) forecast is calculated by running the model with unperturbed initial conditions, and provides a trajectory of the atmospheric state over a period of a few days after the time of the initial conditions. However, taking advantage of the ensemble of perturbed weather forecasts rather than only the deterministic forecast has a significant potential 150 to improve the modelling of ISSRs and upper tropospheric humidity (Hanst et al., 2025). We use ensemble prediction system (EPS) developed by the ECMWF, which is composed of 50 perturbed forecasts (ECMWF, 2024a). The deterministic forecast and all 50 perturbed forecasts are considered equally probable and are produced and available at the same spatial and temporal resolutions. In this study, we do not use the deterministic forecast provided by the ECMWF, reducing the number of members 155 of the ensemble from 51 to 50. As all the forecasts are considered equally probable, we arbitrarily fix the nominal forecast to be the first ensemble member. This nominal forecast will be the one used to optimise flights in the risk-unaware and risk-informed contrail avoidance strategies.

The humidity field of weather forecasts is of first-order importance for predicting the formation and persistence of contrails (Schumann, 1996; Kärcher, 2018). However, when compared with in situ humidity measurements made within the IAGOS research program (Petzold et al., 2015; Boulanger et al., 2018), this field presents significant deviations that hinder the prediction 160 of the formation and persistence of contrails (e.g., Reutter et al., 2020; Gierens et al., 2020; Sausen et al., 2024; Hofer et al., 2024; Hildebrandt et al., 2025). Multiple studies proposed a correction for the humidity field of the ERA5 reanalysis (e.g., Teoh et al., 2022; Platt et al., 2024; Wolf et al., 2025; Wang et al., 2025). In this study, we adopt the humidity correction described by Teoh et al. (2024a). Above a given threshold, relative humidity w.r.t. ice is exponentially boosted, with boosting coefficients that depend on latitude. Although the correction was derived for the reanalysis data, is not re-tuned for the forecast 165 data because the resolution of the forecast we use is the same as that of the reanalysis.

3.3 Aircraft performances, emissions, and climate impact

The performances of aircraft are estimated using the Base of Aircraft Data version 3.15 (BADA3) as provided by EUROCONTROL (EUROCONTROL, 2019). BADA describes changes in aircraft state using a total energy model approach (Nuic et al., 2010; Poles et al., 2010). It provides a framework to accurately estimate the thrust and fuel consumption of aircraft.



170 The total climate impact of an individual flight is quantified using the efficacy-weighted Global Warming Potential over 100 years (EGWP100) CO₂-equivalence metric. This metric was shown to be a suitable metric, to the same extent as the Average Temperature Response over 100 years (ATR100), to quantify and compare the climate impact of the different climate forcers induced by aviation (Megill et al., 2024; Borella et al., 2024). EGWP100 is preferred to ATR100 because it directly derives from the GWP100 metric, which is currently used to report emissions within the United Nations Framework Convention on Climate Change (UNFCCC, 1995, 2019), and there is no strong evidence suggesting that a change of metric is deemed necessary.

175 The species taken into account to calculate the climate impact of individual flights are the emitted CO₂, H₂O, and NO_x, as well as the formed contrails (EASA, 2020). The direct and indirect climate effects of aerosols are neglected in the study, because the magnitudes and signs of these forcings are highly uncertain (Lee et al., 2021). The total climate impact in terms of EGWP100, denoted CLIMATE (in tCO₂e), is calculated from the sum of the contributions from each species:

180
$$\text{CLIMATE} = E_{\text{CO}_2} + \text{EGWP100}_{\text{NO}_x} \cdot E_{\text{NO}_x} + \text{EGWP100}_{\text{H}_2\text{O}} \cdot E_{\text{H}_2\text{O}} + \text{EGWP100}_{\text{AiC}} \cdot \text{EF}_{\text{AiC}} \quad (1)$$

where E_X is the emitted mass of species X (in tons of X), where X stands for CO₂, NO_x, or H₂O. EGWP100_X is the EGWP100 value of the species X (in tCO₂e per tons of X), EF_{AiC} is the energy forcing of the aircraft-induced cloudiness (AiC), i.e., contrails (in J; Teoh et al., 2020), and EGWP100_{AiC} is the EGWP100 value of 1 J originating from contrails (in tCO₂e.J⁻¹).

185 The values of E_{CO_2} , E_{NO_x} , and $E_{\text{H}_2\text{O}}$ are flight-dependent. The fuel is assumed to be Jet A-1 for all aircraft, such that the emission index of CO₂ is $\text{EI}_{\text{CO}_2} = 3.159 \text{ kg}_{\text{CO}_2} \cdot \text{kg}_{\text{fuel}}^{-1}$ and that of H₂O is $\text{EI}_{\text{H}_2\text{O}} = 1.23 \text{ kg}_{\text{H}_2\text{O}} \cdot \text{kg}_{\text{fuel}}^{-1}$ (Wilkerson et al., 2010; Teoh et al., 2024b). The emissions of NO_x are calculated using the Boeing Fuel Flow Method 2 model (DuBois and Paynter, 2006). In this study, we use constant EGWP100 values of NO_x and H₂O. Following Lee et al. (2021) (their Table 5), we fix $\text{EGWP100}_{\text{NO}_x} = 114 \text{ tCO}_2\text{e.tN}^{-1}$ (with 1 tN = 0.304 tNO_x) and $\text{EGWP100}_{\text{H}_2\text{O}} = 0.059 \text{ tCO}_2\text{.tH}_2\text{O}^{-1}$. However, 190 the EGWP100 of NO_x and H₂O are not constant in space and time, but depend on e.g., the location of the emission, the weather pattern, the chemical background conditions (Grewe and Stenke, 2008; Köhler et al., 2013; Frömming et al., 2021). In particular, H₂O emitted in the troposphere has no significant climate impact, contrarily to that emitted in the stratosphere (Forster et al., 2003). The constant factors used for EGWP100_{NO_x} and EGWP100_{H₂O} average these dependencies over the entire aviation sector.

195 The energy forcing of contrails, EF_{AiC}, is calculated using CoCiP, a Lagrangian model that simulates the formation, evolution, and radiative impact of contrail cirrus on flight segments based on aircraft emissions and atmospheric conditions (Schumann, 2012). It accounts for processes such as ice crystal formation, sedimentation, dispersion, and radiative transfer, enabling the estimation of contrail energy forcing along a flight trajectory. The model requires non-volatile particulate matter (nvPM) emissions along the aircraft trajectory as an input. These are estimated using the ICAO Aircraft Emissions Databank 200 (EASA, 2025). For this study, we use the CoCiP version that was adapted for Python in the `pycontrails` package, version 0.54.6 (Shapiro et al., 2025). The nominal predicted energy forcing of contrails is estimated using the default parameters of `pycontrails` and the nominal weather forecast.

We use the GWP100 of emitting 1 J of contrails calculated by Borella et al. (2024) using the OSCAR model (Gasser et al., 2017), with $\text{GWP100}_{\text{AiC}} = 8.5 \times 10^{-13} \text{ tCO}_2\text{e.J}^{-1}$. This value is scaled by the climate efficacy of contrails, set to 0.37 (Borella et al., 2024), so that $\text{EGWP100}_{\text{AiC}}$ is $3.1 \times 10^{-13} \text{ tCO}_2\text{e.J}^{-1}$. We emphasise that the estimate of the climate efficacy of contrails is associated with a very significant uncertainty, as reaffirmed by Bickel et al. (2025). However, as this uncertainty is not weather-related, or at the very least cannot be quantified at the local level, we do not consider it in this study, and consider the climate efficacy of contrails to be the same for all flights.

Instead of estimating only a nominal predicted energy forcing from CoCiP, we consider an ensemble of CoCiP predictions of the contrail energy forcing that sample parametric uncertainties of the model. The ensemble is built by varying seven key parameters within their plausible ranges through a Monte Carlo approach and estimating the corresponding energy forcings (Platt et al., 2024). The parameters are the initial wake vortex depth, the wind shear enhancement exponent, the sedimentation impact factor, the scaling factors for shortwave and longwave radiation, a scaling factor for the number emission index of nvPM, and the habit weight mixtures. An in-depth physical description of these parameters has been made by Schumann et al. (2012) and Schumann (2012). From the range of each parameter, we generate 70 different configurations using a Monte Carlo approach (10 times the number of varied parameters), in addition to the nominal configuration. For each flight trajectory, CoCiP is run with these 71 configurations, resulting in a distribution of predicted contrail energy forcing values. This approach allows us to propagate the uncertainty of each parameter into an uncertainty for the contrail energy forcing. Such an uncertainty is hereinafter referred to as the CoCiP-based uncertainty, with the associated CoCiP-based variability.

Following the same Monte Carlo approach, we can also estimate the uncertainty that stems from the weather forecast, by calculating the predicted climate impact of contrails for each of the 50 perturbed forecasts. The resulting uncertainty is hereinafter referred to as the weather-based uncertainty, with the associated weather-based variability. To take into account both the CoCiP-based and the weather-based uncertainties, we also calculate a joint uncertainty that corresponds to the total potential climate benefit calculated using all the 71 CoCiP configurations for all the 50 weather forecast ensemble members, resulting in 3550 estimates for each flight. The associated variability is hereinafter referred to as the joint variability. The average predicted climate impact of contrails refers to the average of all the estimates of the Monte Carlo process.

3.4 Flight planning and optimisation

The full 4D trajectories of the flights are not available from the FlightRadar24 database available to us, and must therefore be reconstructed. Similarly, the alternative routes that would lead to contrail avoidance must be created. To this end, we adopt in this study a flight planning approach and optimise trajectories taking into account the weather, the aircraft performance and fuel requirements, the flight duration, as well as its climate impact.

One of the main objective of flight planning is to minimise the operating cost of an aircraft. For a given aircraft, this can be roughly approximated by a linear function of flight time and fuel consumption. The flight can also be given a climate cost noted CLIMATE (Eq. 1). The total cost function to minimise is therefore:

$$235 \quad \text{COST} = \phi_0 + \phi_t \cdot \text{TIME} + \phi_f \cdot \text{FUEL} + \phi_c \cdot \text{CLIMATE} \quad (2)$$



where COST quantifies the costs of the flight for the airline (in USD), TIME is the flight time of the aircraft (in s), and FUEL is the fuel consumption (in kg). The ϕ_x coefficients correspond to the conversion factors between physical and monetary units. ϕ_0 quantifies to the fixed costs (in USD) of a flight but since it is constant, it has no impact on the minimisation of the cost function. Thus, it is arbitrarily set to $\phi_0 = 0$ USD. We fix the cost of fuel ϕ_f to 0.51 USD.kg⁻¹, and that of time ϕ_t to 0.51 USD.s⁻¹.
240 While these values are realistic (Yamashita et al., 2020), we emphasise that the actual cost of the flight has no importance in our work, and that only the relative weights of each contribution are impactful. The cost of climate impact ϕ_c depends on the the routing strategy. If the climate impact is not taken into account, as it is currently done in operational flight planning, ϕ_c is set to 0 USD.tCO₂e⁻¹, and the resulting cost-optimal route is called the default route. On the contrary, the alternative route
245 is determined by setting ϕ_c to a positive non-zero value of 10 USD.tCO₂e⁻¹, to determine a cost climate-optimal route. This value can be lowered to reduce the relative importance of climate in the cost function, or increased to increase it.

The optimisation tool we use for this study is FlightOptima, a software that evolved from that described by Boucher et al. (2023). FlightOptima finds the optimal route between two points, minimising the cost function defined in Eq. 2. We account for basic ATC rules by imposing that westbound flights cruise at odd levels (i.e., 31000 ft, 33000 ft, 35000 ft, etc.), and that eastbound flights cruise at even levels (i.e., 30000 ft, 32000 ft, 34000 ft, etc.). Moreover, we impose that aircraft cannot execute
250 more than one climb or descent step every 400 km. However, the aircraft flies in free routing on the horizontal plane, with no ATC constraint. For the purpose of this study, we impose the speed schedule of aircraft, such that they are flying at constant Mach number during cruise. Specific implementation details of FlightOptima are proprietary and cannot be disclosed due to its intellectual property status. We emphasise that we do not investigate in this study the feasibility and potential gains of contrail avoidance, but the decision-making linked to the risks of unintentionally damaging the climate when flying alternative routes.

255 For the purpose of the optimisation process, the energy forcing of contrails is determined using the gridded version of CoCiP, CoCiPGrid (Engberg et al., 2025), which allows to estimate the predicted climate impact of an aircraft that would fly in a specific gridbox. The horizontal resolution of the model is the same as that of the weather data, and the vertical grid corresponds to all the flyable flight levels (that is, both odd and even levels). Moreover, only warming contrails are considered during the optimisation process, as to avoid the rerouting of flights to create cooling contrails. The full impact of contrails,
260 cooling and warming, is taken into account in the results presented in this study. If an alternative route would have a total predicted climate impact higher than the default route, typically because cooling contrails formed on the default route, the alternative route is overridden by the default route and no rerouting option is possible.

4 CoCiP- and weather-based variability for two case studies

In this section, we investigate the variability of the predicted climate impact of contrails using two specific flights of the flight
265 data subset, called flights A and B. They were selected because they have both a high predicted climate impact and similar fuel consumption, while their associated uncertainties are very different. The cost-optimal and cost climate-optimal routes are both calculated using the nominal weather forecast and nominal CoCiP configuration. By estimating the risk of unintentionally damaging the climate during rerouting, the risk-unaware and risk-informed strategies are compared.



4.1 Description of the default and alternative routes

270 Flight A flown from New York (KJFK) to London (EGLL) departed at 00:51 UTC on 5 March 2024 and was carried out by a Boeing 777-300ER aircraft. From this data and from the weather forecast operational archive, the trajectory is reconstructed by minimising operating costs (Fig. 3). The trajectory follows the jet stream without deviating too much from the orthodromic path (i.e., the shortest route), while changing once its cruising altitude as it gets lighter. In total, the aircraft consumed 47.7 t(fuel) and the predicted nominal climate impact of the flight, calculated using from the nominal weather forecast and nominal CoCIP 275 configuration, was 288 tCO₂e, amongst which contrails contributed 128 tCO₂e. This is because the aircraft flies within a region prone to highly-warming contrail formation (red patches on Fig. 3). An alternative route is calculated by minimising total costs, including both operating costs and climate costs (Fig. 3). The alternative trajectory, called rerouting A, avoids the highly-warming contrail formation region by flying below. The rest of the trajectory is almost identical to the default route. We emphasise that this avoidance is the most optimal avoidance given the conditions described in Section 3. When flying the 280 alternative route, the aircraft consumes more fuel with a total of 48.2 t(fuel), representing an increase of 1.0% compared to the default route, because the flight deviates from its cost-optimal route. However, the flight time is slightly lower by 15 s, but this reduction is insignificant compared to the total flighttime of 6 hours and 3 minutes. Most importantly, the total predicted climate impact is reduced by 43.2% to 164 tCO₂e. The contribution from contrails is reduced by 98.6% to 2 tCO₂e, confirming that the cost-climate optimised flight avoids the regions prone to highly-warming contrail formation.

285 Flight B flown from London (EGLL) to Newark (KEWR) departed at 15:51 UTC on 15 December 2024 and was carried out by a Boeing 767-300ER aircraft. As the flight is westbound, it faces the dominant winds. As a consequence, the cost-optimal trajectory avoids the strongest headwinds while again following as close as possible the shortest route. The flight duration is also longer than for flight A by about 1 hour and 15 minutes. Just like flight A, the aircraft climbs during its journey as it gets lighter. During its journey, the aircraft consumed 34.8 t(fuel) and its predicted nominal climate impact was 275 tCO₂e, contrails 290 being responsible for 165 tCO₂e. The most warming contrails are predicted to be formed around halfway through the flight. The region prone to highly-warming contrail formation extends vertically on multiple flight levels and is roughly orthogonal to the flight trajectory, making it difficult to avoid. The alternative trajectory, called rerouting B, avoids the region by shifting to the north. This wide horizontal avoidance increases the flight duration by 0.6%, or 160 s, compared to flying the default route. However, as the flight level is still optimum, the increase in fuel consumption is lower than for rerouting A, at 0.3%, for a total 295 consumption of 34.9 t(fuel). The reduction in total climate impact is similar to that of rerouting A, as the total predicted climate impact of rerouting B is 124 tCO₂e, representing a 54.9% decrease. The corresponding contrail climate impact is reduced by 93.3%, down to 11 tCO₂e.

300 Flights A and B have similar characteristics and fuel consumption, and using nominal prediction of the climate impact of the formed contrails, the potential reduction in total climate impact of each individual flight is also similar, at about 50%. The total predicted climate benefit for flight A is 125 tCO₂e, while it is 151 tCO₂e for flight B, indicating a potential major opportunity for the reduction of climate impact of these flights at a very limited cost. If the risk-unaware contrail avoidance strategy is

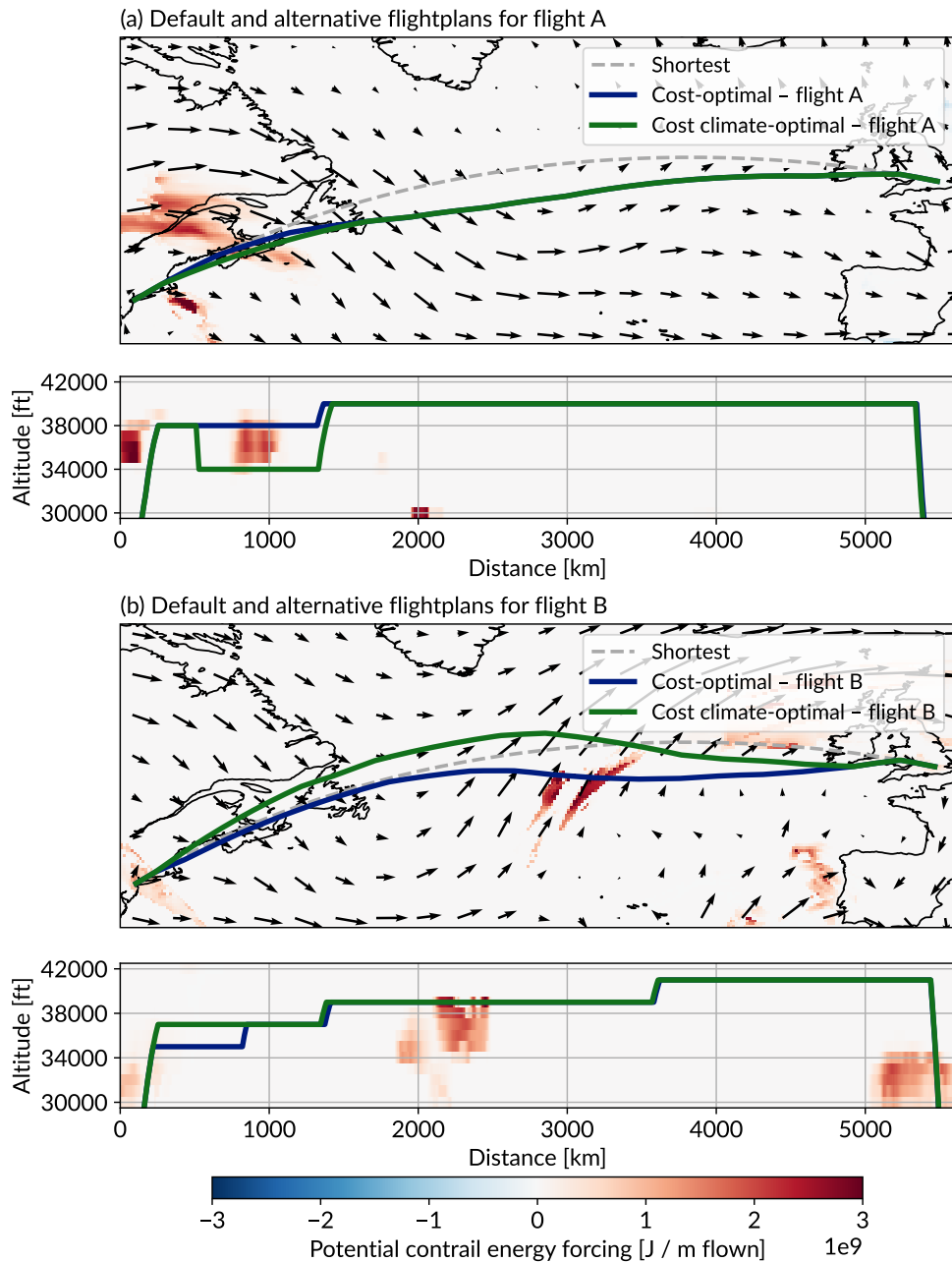


Figure 3. Horizontal and vertical flight plans of the default cost-optimal route (blue lines) and alternative cost climate-optimal route (green lines) for (a) flight A and (b) flight B. Colors indicate the predicted potential contrail energy forcing (in J/m flown) calculated by CoCiPGrid, with the arrow field depicting the winds. The level and timestamp of the color shade and arrow field are those of the aircraft. Basemap plotted using Cartopy 0.22.0 and sourced from Natural Earth.

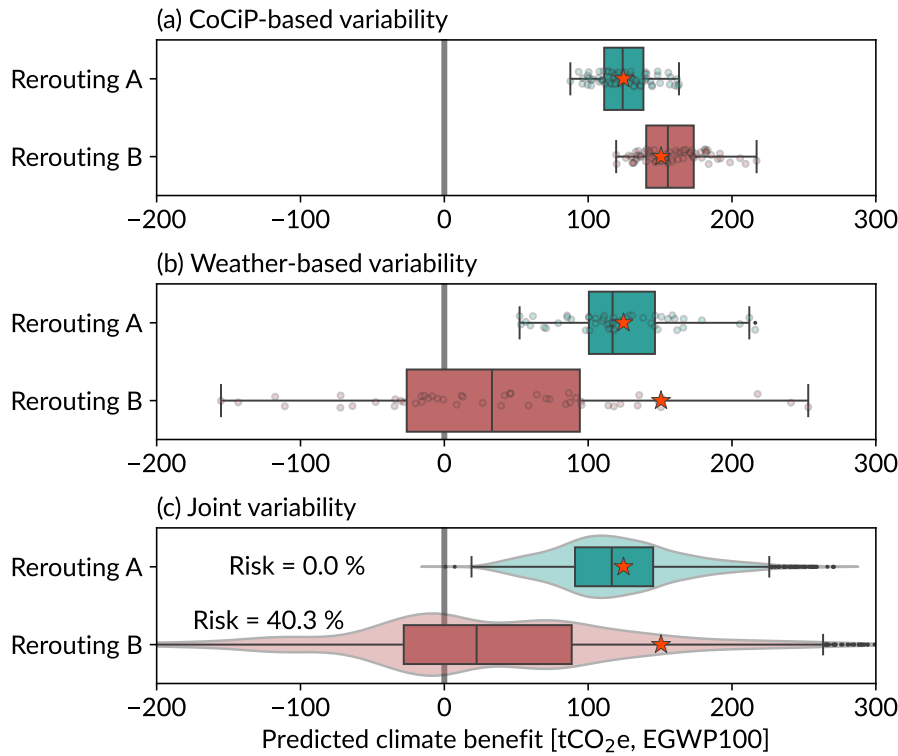


Figure 4. (a) CoCiP-based, (b) weather-based, and (c) joint variability of the total predicted climate benefit (in tCO₂e, EGWP100) for two flights between a cost-optimal route and a cost climate-optimal route. The red stars indicate nominal total predicted climate benefit for the two reroutings.

adopted, the decision-making is reduced to ensuring that the climate benefit is positive, as the maximum acceptable costs of avoidance are already included in the optimisation process.

4.2 Variability of the predicted climate benefit

305 The CoCiP-based, weather-based, and joint variability of the predicted climate benefit are estimated for both flights. The 71 configurations of CoCiP, as well as the 50 ensemble members of the weather forecast, are used as inputs of the Monte-Carlo process. We recall that both the cost-optimal and the cost climate-optimal routes are calculated using the nominal weather forecast and CoCiP configuration.

310 The CoCiP-based variability of the predicted climate benefit ranges from 88 to 163 tCO₂e for flight A, representing a relative difference to the nominal estimate between -30 and 30%, and for flight B ranges from 119 to 217 tCO₂e, with a corresponding relative range of -21 to 44% (Fig. 4a). The nominal estimate is for both flights close to the median and the average of the Monte Carlo ensemble, respectively equal to 125, 124, and 125 tCO₂e for flight A, and 151, 155, and 159 tCO₂e for flight B. For flight A, the variability in the estimation mainly originates from the parameter controlling the enhancement of wind shear,



and to a lesser extent to that controlling the enhancement of nvPM emissions (not shown). Moreover, the parameter controlling
315 the enhancement of longwave radiative forcing plays a slight role. For flight B, the nominal estimate is strongly sensitive to the parameter controlling the enhancement of nvPM emissions, but shows no strong dependence on any other parameter.

The weather-based variability is significantly higher than the CoCiP-based one (Fig. 4b). For flight A, the estimate can be reduced by 58% or increased by 73% compared to the nominal estimate, depending on the ensemble member. For flight B, the lowest estimate of climate benefit becomes negative, with a corresponding decrease of 239% compared to the nominal
320 estimate. This implies that if the actual weather was close to that of the ensemble member leading to this low estimate, flying the alternative route would damage the climate. This is in fact the case for 21 ensemble members out of 50, indicating that flying the alternative route rather than the default one would damage the climate in 42% of the weather scenarios. Moreover, the average and median values can be very different from the nominal estimate of the total potential climate benefit. Contrarily to the CoCiP-based variability, where the nominal value is calculated from the selection of central estimates for each parameter,
325 the nominal value estimated for the weather forecasts does not originate from the selection of a ‘central’ weather forecast. As all the 50 forecasts are considered to be equally probable, there is no best guess, and the nominal ensemble member is chosen arbitrarily. This can therefore lead to nominal estimates that are very different from the median or average estimates, as it is the case for flight B.

The distribution of the predicted climate benefit considering the joint variability is similar to that considering only the
330 weather-based variability for both flights (Fig. 4c). The conclusions are therefore similar: for flight A, the nominal predicted climate benefit and the average and median values calculated from all the estimates are similar, and all these estimates are positive. For flight B however, 40.3% of the estimates of predicted climate benefit are negative, although the nominal benefit is positive and high. Moreover, the nominal benefit and the average and median benefits are very different, the latter two being close 25 tCO₂e.

335 The joint variability quantifies the distribution of potential climate benefit when a flight is rerouted when considering uncertainties in predicting the climate impact of contrails, and can be used to inform decision-making on contrail avoidance. When the variability is not estimated, decision-making is reduced to ensuring that the nominal benefit is positive so that the rerouting is beneficial for the climate. We refer to this strategy as the risk-unaware avoidance strategy.

When the joint variability is calculated, the risk of unintentionally damaging the climate can be estimated, corresponding
340 to the proportion of estimates of total predicted climate benefit that are negative. For flight A (resp. B), this estimated risk is therefore of 0% (resp. 40.3%) if the aircraft flown the alternative route. Providing this value for decision-making is key, in particular for a no-regret avoidance policy for which it is better to do nothing rather than mistakenly damage the climate. If the risk-unaware avoidance strategy was adopted, both flights A and B would be rerouted, although there would be an, unquantified, significant risk of damaging for flight B. If the risk-informed avoidance strategy was adopted, flight A would still be rerouted,
345 but flight B would likely not, in particular in the context of a no-regret avoidance policy. The average climate benefit would therefore be lower, but the confidence in the success of each individual rerouting would be significantly improved.

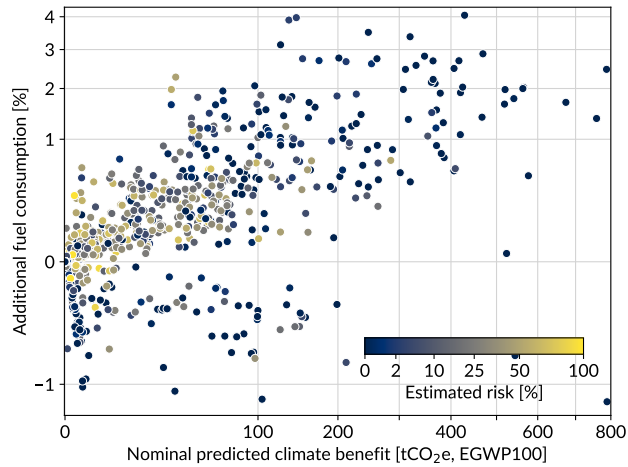


Figure 5. Additional fuel consumption needed to reroute the flight (in %) against nominal predicted climate benefit (in tCO₂e, EGWP100) for the 641 reroutings. Colors indicate estimated risk of unintentionally damaging the climate due to the misprediction of contrail forcing (in %).

5 Risk-informed avoidance strategy applied to a small fleet

In this section, the risk of unintentionally damaging the climate is analysed for the 1747 transatlantic flights distributed across the seasons of 2024. In total, these flights consumed 71,579 t(fuel), and 1364 formed persistent contrails amongst which 1067 350 formed warming ones. The total predicted climate impact of the formed warming contrails is 54,755 tCO₂e, while that of all the persistent contrails is 52,414 tCO₂e, showing the small contributions of cooling contrails. In total, the 1747 flights are predicted to have warmed the climate by 287,956 tCO₂e, with contrails contributing to 18% of the total climate impact, in line with previous assessments (Teoh et al., 2024a; Martín Frías et al., 2024).

355 Applying the risk-unaware avoidance strategy, all the flights for which an alternative route with positive total predicted climate benefit exists are rerouted, corresponding to 672 flights or 38% of the total number of flights. This number is lower than the number of flights forming warming contrails, because the flight planning tool does not minimise the climate impact but the cost including the climate impact, such that flights forming low-warming contrails are not rerouted. The total fuel consumption increases by 0.14% (99 t(fuel)), representing an average of 0.35% (0.15 t(fuel)) for the rerouted flights. The predicted reduction of the total climate impact is 17% (49,141 tCO₂e), or 23% (73 tCO₂e) on average for a rerouted flight. 360 The contribution from contrails is overall reduced by 95% (49,540 tCO₂e). These significant reductions are expected, since the optimisation was conceived to minimise the climate impact and additional fuel consumption, and that it was previously shown that this minimisation could be done with a limited cost increase (e.g., Simorgh and Soler, 2025; Zengerling et al., 2024).

365 For each rerouted flight, the risk of unintentionally damaging the climate is estimated (Fig. 5). 24% of the reroutings (164 flights) present no risk of damaging the climate, complying with a no-regret avoidance policy. For the other reroutings, the risk can be as high as 98%. However, the level of estimated risk relates to the nominal predicted climate benefit,

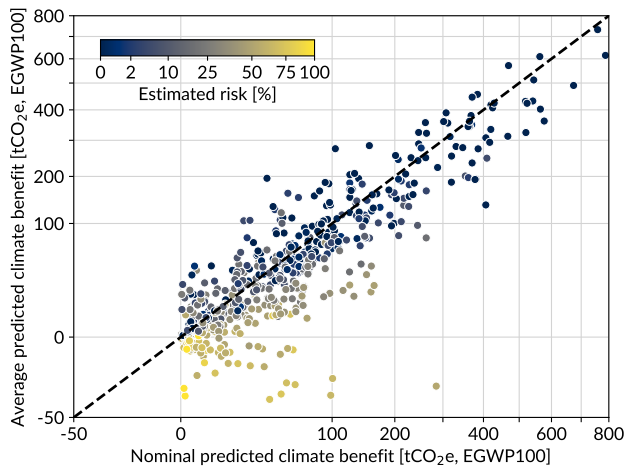


Figure 6. Average predicted climate benefit against nominal predicted climate benefit (both in tCO₂e, EGWP100) for the 641 reroutings. Colors indicate the level of risk associated with each rerouting (in %).

such that avoiding the formation of highly warming contrails is often low-risk, high-benefit. The corresponding cost-optimal trajectory can be characterised as ‘big hits’. The reroutings associated with these high nominal predicted climate benefit are also correlated to a higher additional fuel consumption, because the corresponding cost-optimal flights are characterised by a crossing of an often large highly-warming contrail-forming region. The alternative route therefore takes a significant detour
 370 to avoid this region, such that the additional fuel consumption is high, and the predicted climate benefit is high. Because of the long detour, the risk of unintentionally damaging the climate associated with the weather-based variability is lower. This is because ice supersaturated regions are globally well predicted by weather forecasts, but these are often slightly shifted in space or time compared to the actual location of the region (Dean et al., 2025). Taking a long detour avoids the forecasted region in all the members of the ensemble. These results indicate that, while risks of unintentionally damaging the climate should be
 375 taken into account in contrail avoidance strategies, ‘big hits’ can still be avoided with a relatively low-level risk.

In addition to estimating the risk of unintentionally damaging the climate, calculating the variability of the predicted climate benefit for each rerouting makes it possible to derive an average predicted climate benefit rather than a nominal one. The average values is a better predictor of the potential benefit than the nominal value, as the latter is estimated using nominal conditions corresponding to an arbitrary ensemble member of the weather forecast. As expected, the average value is globally
 380 similar to the nominal value, following the 1:1 line (Fig. 6). However, the average value can be significantly lower than the nominal one, and below 0 in some cases. These strong deviations are correlated to high risk levels, especially for low nominal predicted climate benefits. For high nominal predicted climate benefits, although the average value can be lower than the nominal value, the benefit is always substantial and the risk is in most cases close to 0%. This again indicates that ‘big hits’ can be avoided with a limited risk of unintentionally damaging the climate, and that the expected climate benefit is not too different
 385 to the nominal predicted climate benefit.

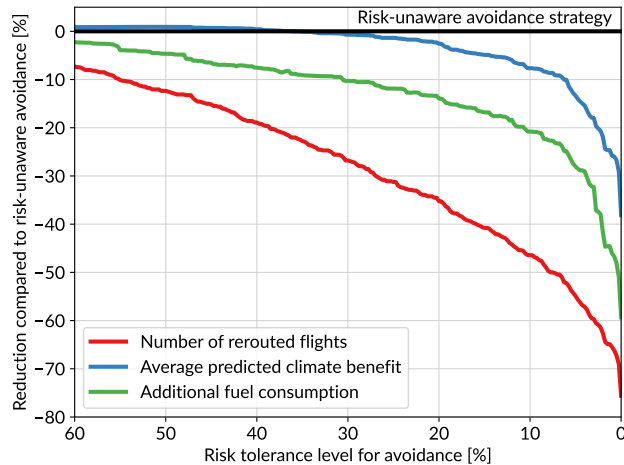


Figure 7. Reduction in number of rerouted flights (red line), average predicted climate benefit (blue line), and additional fuel consumption (green line), of a risk-informed avoidance strategy compared to the risk-unaware avoidance strategy (black line), as a function of the risk tolerance level (in %).

By adopting the risk-unaware avoidance strategy, there is a significant risk of unintentionally damaging the climate for multiple potential reroutings. On the contrary, adopting the risk-informed avoidance strategy allows to use the calculated variability to confine this risk below a given risk tolerance level. The no-regret avoidance policy is adopted if the tolerance level is set to 0%. As expected, the number of flights that would be rerouted decreases with decreasing risk tolerance level 390 (Fig. 7). When adopting a no-regret avoidance policy, the number of rerouted flights is reduced by 76% compared to adopting the risk-unaware avoidance strategy. The average predicted climate benefit is in this case reduced by 38%, such that the total average predicted climate impact for the entire 1747 flights is reduced by 9%. The lower benefit compared to the risk-unaware avoidance strategy, within which the total average predicted climate impact is reduced by 14%, is a trade-off with an increased confidence in the fact that each individual rerouting does actually benefit the climate. By relaxing the risk tolerance level 395 from 0% to for example 5%, the decision-making consists of rerouting flights for which the risk of unintentionally damaging the climate is below 5%. In this case, 303 flights are rerouted for an average predicted climate benefit of 35,192 tCO₂e, representing a reduction compared to the risk-unaware avoidance scenario in 55% of the number of rerouted flights and in 13% of the average predicted climate benefit. As expected, the additional fuel consumption reduces similarly to the number 400 of rerouted flights and that of average predicted climate benefit because the most risky reroutings are likely consuming less additional fuel than the less risky ones (see Fig. 5), and they also have a near-insignificant role on the average predicted climate benefit. The average predicted climate benefit is slightly higher for risk-informed strategies than for risk-unaware strategies because reroutings that are on average damaging the climate are not rerouted anymore.



6 Optimising the risks during the flight planning process

405 In this section, we investigate how the risk-optimised strategy can be used to both increase the confidence that single reroutings will not unintentionally damage the climate, as for the risk-informed avoidance strategy, while avoiding the large decrease in potential climate benefit seen when adopting a no-regret avoidance policy for the risk-informed avoidance strategy. To decrease computational costs, this section relies only on the weather-based uncertainty, but the qualitative conclusions are not affected when using the joint uncertainty instead.

410 First, the risk-optimised avoidance strategy is pictured using the two flights from the previously described case study (Fig. 8). For both flights, the cost-optimal route is weakly sensitive to the selected ensemble member, such that the 50 cost-optimal routes are very similar. However, the 50 cost climate-optimal routes can be very different. For flight A, the differences are mostly concentrated on the altitude descent needed to avoid the warming contrail-forming region, indicating the uncertainty in predicting the altitude of this region. For flight B, the different routes are much more spread out, as expected from the larger 415 weather forecasts variability for flight B than for flight A. Three clusters of routes can be identified, one avoiding the main warming contrail-forming region by the south, one by the north, and one by flying below.

420 The weather-based variability is then computed for the 50 trajectories (Fig. 9). The envelope around the average benefit quantifies the range of predicted climate impact of the flight from the 50 ensemble members of the weather forecast. For flight A, the variability in the predicted climate benefit is similar for all trajectories. This is also the case for the additional fuel consumption needed to fly the alternative route compared to the default route, which is roughly increasing with increasing average. This is because for low average benefits, the trajectory avoids warming contrail-forming regions by flying very close to them, such that the additional fuel consumption is low. However, in most of the ensemble members, this route leads to the formation of a warming contrail, because the region is predicted to be slightly shifted in space or time, such that the route that was predicted to be highly beneficial for the climate in one member leads to lower benefits in other members. It is the 425 other way around for high average benefits, whereby the trajectory widely avoids the contrail-forming regions. The decision of which alternative route to consider given a risk tolerance level consists of choosing the route with the highest average climate benefit amongst those for which the 5th percentile, if the risk tolerance level is set to 5%, is positive. By choosing such a route, we both guarantee that the risk of unintentionally damaging the climate is lower than 5%, and that the route has the highest predicted potential for climate benefit. For flight A, this corresponds to the route on the very right of the plot (Fig. 9a).

430 For flight B, three regimes can be observed (Fig. 9b), roughly corresponding to the three clusters mentioned above (Fig. 8b). The first one groups routes that have a small climate benefit and a small envelope. These routes are mostly located on the left of the plot, and are associated with low additional fuel consumptions. They correspond to routes that are very similar to the default route, with almost no deviation and no average climate benefit. The second regime groups routes with an intermediate average climate benefit, a wider envelope than for the first group, but a significant higher additional fuel consumption, globally 435 located in the middle of the plot. Finally, the routes on the right side of the plot are those with the highest potential for climate benefit and, at the same time, they are the only routes for which the 5th quantile is positive. For flight B, the best route

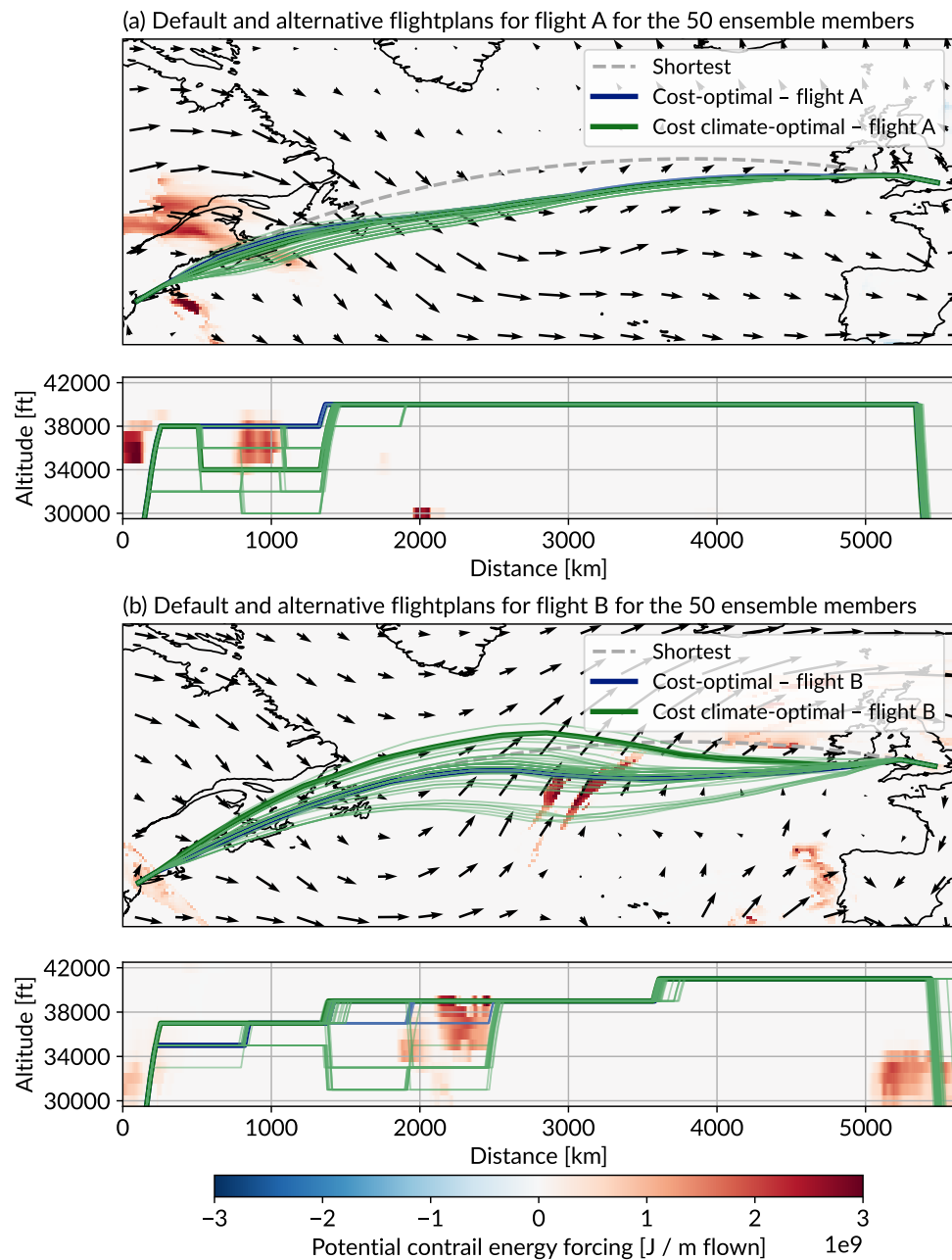


Figure 8. Same as Fig. 3 but with the optimisation ran for the 50 ensemble members of the weather forecast for both cost-optimal routes (thin blue lines) and cost climate-optimal routes (thin green lines). The variations in cost-optimal routes can hardly be seen as they are almost all stacked. Basemap plotted using Cartopy 0.22.0 and sourced from Natural Earth.

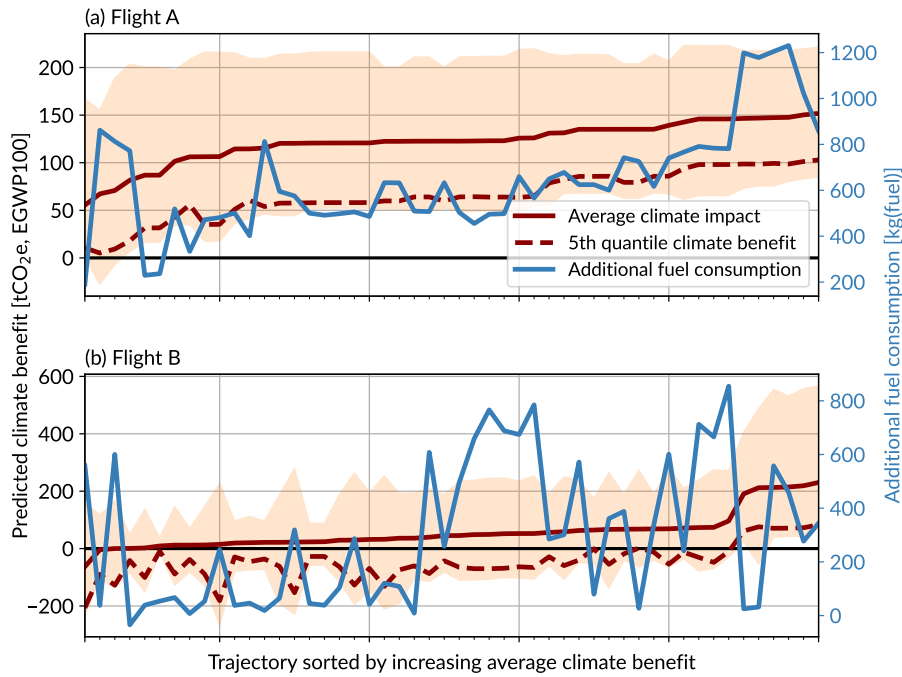


Figure 9. Weather-based variability of the predicted climate benefit (in tCO₂e, EGWP100) for the 50 cost climate-optimal routes determined from the 50 ensemble weather forecast members. The statistics shown are the average (red line), the 5th quantile (dashed red line), and the minimum and maximum values (orange shading). The additional fuel consumption (in kg(fuel)) needed to fly the trajectory compared to the cost-optimal route is also shown (blue line).

again corresponds to that on the right of the plot (Fig. 9b). However, we emphasise that high average climate benefits are not necessarily correlated with low risks.

The potential benefits of adopting the risk-optimised avoidance strategy are compared to that adopting the risk-informed avoidance strategy, using the risk-unaware avoidance strategy as a reference (Fig. 10). The average predicted climate benefit is much higher for the risk-optimised strategy than for the risk-informed one. It is also higher than the risk-unaware strategy for all the risk tolerance levels, increasing the benefit by 52% for a no-regret avoidance policy which corresponds to the 0% risk tolerance level. This is because the alternative route is chosen amongst 50 possibilities rather than only one, allowing flexibility in the choice of route. When the risk tolerance level decreases, the selected cost climate-optimal route can change so as to increase the confidence in the rerouting. In this case, the average predicted climate benefit is decreased but the flight is still deviated to take a cost climate-optimal route. This is shown by the higher number of rerouted flights, increased by 57% compared to the risk-unaware strategy when adopting a no-regret avoidance policy. On the contrary, the flight would simply fly the cost-optimal route rather than being rerouted if the risk-informed avoidance strategy were to be adopted. Adopting such a strategy and a no-regret avoidance policy leads to a reduction of the number of rerouted flights by 65% compared to the risk-unaware strategy, and of the average climate benefit by 24%. In total, 238 flights would be rerouted by adopting the

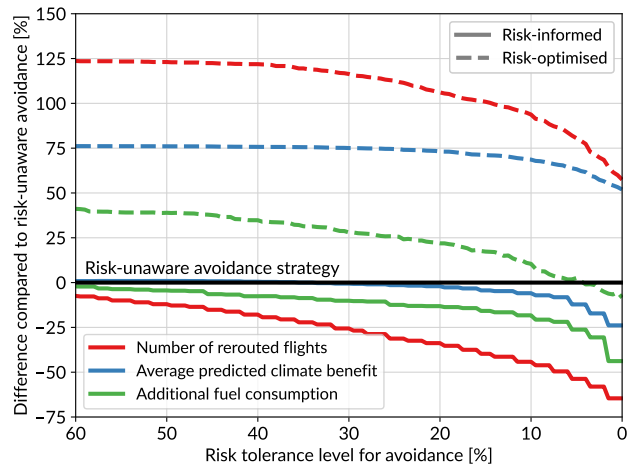


Figure 10. Reduction in number of rerouted flights (red lines), average predicted climate benefit (blue lines), and additional fuel consumption (green lines), of a risk-informed (full lines) and a risk-optimised (dashed lines) avoidance strategy compared to the risk-unaware avoidance strategy (black line), as a function of the risk tolerance level (in %). Only the weather forecasts variability is taken into account.

risk-informed avoidance strategy with a no-regret avoidance policy, for a total benefit of 31,144 tCO₂e and an additional fuel consumption of 56 t(fuel). For the risk-optimised avoidance strategy with a no-regret avoidance policy, 1058 flights would be rerouted, leading to a total benefit of 62,153 tCO₂e and an additional fuel consumption of 91 t(fuel).

7 Discussion and conclusion

455 Uncertainties in estimating the climate impact of contrails present a challenge for the targeted contrail avoidance strategy, as the nominal estimate of the climate impact can often be an outlier in the associated uncertainty distribution. This indicates that the estimation of the climate benefit of reroutings must not be reduced to using only one deterministic modelling configuration. Moreover, a rerouting that was initially predicted to benefit the climate could in fact cause unintended climate damage. The risk of unintentionally damaging the climate for a given flight may be acceptable if avoiding contrails leads to a climate 460 benefit when averaged over a fleet. But initially, in a ramp-up phase of contrail avoidance, we may want to limit the risk for every single rerouting. Informed decision-making on whether to reroute a flight or not should therefore include the risk of unintentionally damaging the climate (Niklaß et al., 2024). Such a consideration calls for flight planning systems to consider as many uncertainties as scientifically possible and the potential negative outcome of reroutings.

To take the risk of unintentionally damaging the climate into account, two risk-aware strategies are investigated. The risk-465 informed avoidance strategy consists of applying an analysis of the variability of the predicted climate benefit once cost-optimal and cost climate-optimal routes are calculated. If the cost climate-optimal route presents a risk of unintentionally damaging the climate above a given threshold, the cost-optimal route is flown instead. The risk-optimised avoidance strategy includes the uncertainty in the prediction of the climate impact of contrails directly in the flight planning process, but comes with a



470 greater computational cost and operational constraints. For both strategies, an increased certainty in the positive outcome of reroutings comes with a decreased potential in climate benefit, as less flights are rerouted. However, the most risky reroutings are also those associated with a low average benefit. The ‘big hits’, namely the reroutings which can lead to a substantial climate benefit, are globally much less affected by risks of damaging the climate than other reroutings. When adopting the risk-optimised avoidance strategy rather than the risk-informed one, the risk of unintentionally damaging the climate is directly included when selecting the potential alternative route. Thus, the potential climate benefit is higher for the same risk tolerance 475 level, as many more flights can be rerouted. In any case, our study demonstrates that the risk of unintentionally damaging the climate should be integrated into the decision-making of contrail avoidance, in particular if a no-regret avoidance policy is to be adopted.

480 The risk of unintentionally damaging the climate investigated in this study is calculated from the parametric uncertainty of the CoCiP model (Schumann et al., 2012; Schumann, 2012; Platt et al., 2024) and from that of the weather forecasts of the IFS (ECMWF, 2024a). Although we used a weather forecasting framework, which is similar to operational conditions compared to the commonly used reanalysis framework, many uncertainties on the prediction of the climate impact of contrails were not considered. An important one is the value of the climate efficacy of contrails, which scales the predicted climate impact of contrails. The best estimate is derived from only three independent studies, which each estimate being very different one from another, at 0.21, 0.31 and 0.59 (Ponater et al., 2005; Rap et al., 2010; Bickel et al., 2025). Bickel et al. (2025) found that 485 their 0.21 estimate is associated with a statistical uncertainty between 0.10 and 0.32. This uncertainty has a major role on the potential benefit of the contrail avoidance strategy. The average predicted climate benefit for a risk-informed strategy, using a 5% risk tolerance, linearly depends on contrail efficacy, such that the advantage of contrail avoidance could be reduced by 80% if contrail efficacy was equal to 0.10 on average (Fig. 11). However, the number of flights that should be rerouted, as well as the additional fuel consumption needed to fly these deviations, are much less sensitive to contrail efficacy. This indicates that 490 not only the potential climate benefit, but also the efficiency of contrail avoidance both in terms of costs and complexity, is linearly dependent on contrail efficacy, emphasizing the need for additional work in this field.

495 Another source of uncertainty comes from the structural limitations of CoCiP, which were not considered in this study. Compared to APCEMM, a model similar to CoCiP but with increased physical complexity (Fritz et al., 2020), CoCiP was found to underpredict lifetime optical depth (Akhtar Martínez et al., 2025). Other models are also modelling the impact of contrails (e.g., Yin et al., 2023). Simorgh et al. (2024a) conceptualised a way to plan flight routes under multiple estimates of contrail climate impact, but it is clear that these models need to be evaluated more systematically between themselves, and most importantly against observations. In particular, in order for our risk-aware decision-making to be valid, the actual climate benefit of a rerouting should lie within the estimated variability. This is still an open question that needs to be addressed. We 500 strongly advocate for additional research in evaluating and verifying CoCiP and similar models against observations, which may be used for operational contrail avoidance. Until then, a first step would be to assess whether the climate benefit estimated using reanalysed meteorological data falls within the estimated variability, which will be the subject of future work.

Moreover, our study did not consider the variability in the climate impact of the emissions of NO_x and H₂O, which depends on e.g., the location of the emission, weather pattern, and chemical background conditions. To account for these dependences,

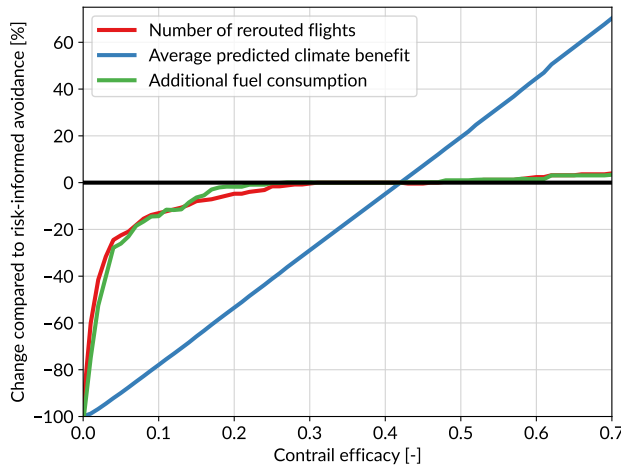


Figure 11. Reduction in number of rerouted flights (red line), average predicted climate benefit (blue line), and additional fuel consumption (green line), of a risk-informed avoidance strategy (at a 5% risk tolerance level) with contrail efficacy varying between 0 and 0.7, compared to the same situation with contrail efficacy fixed to 0.42 (black line).

van Manen and Grewe (2019) derived algorithmic climate change functions (aCCFs) from spatiotemporal variation of the 505 globally-average climate impact from a local emission (Grewe et al., 2014). These aCCFs had been used in multiple climate-friendly flight planning studies (e.g., Rao et al., 2022; Simorgh et al., 2023; Yin et al., 2023; Castino et al., 2024). We did not use them in this study as the focus was on contrails to better illustrate our risk-aware framework, but future work could include weather- and location-dependent formulations of the EGWP100 of NO_x and H₂O. In addition, there remains a need for flight-by-flight models able to estimate the climate impact of aerosol interactions with radiation and clouds.

510 Better integrating the different sources of uncertainties in flight planning systems should be investigated for future operational trials of contrail avoidance. Moreover, uncertainties should not only be considered for mitigation purposes, but more generally when estimating the potential climate impact of contrails. Finally, we emphasise that the targeted contrail avoidance strategy can provide a crucial additional time to the aviation sector to reduce its CO₂ emissions, but should not be considered a decarbonation strategy on its own.

515 *Data availability.* Data used for the analysis and plots will be made available on Zenodo upon acceptance. IFS forecast data were retrieved from the MARS Operational archive database.

Author contributions. AB, CS, and OB conceptualised the study. CS ran the simulations and performed the data analysis and evaluation of preliminary results. AB ran the simulations, performed the data analysis and evaluation of the results, and drafted the manuscript. All authors have read, reviewed, edited, and agreed upon all contents of the paper.



520 *Competing interests.* AB and OB are founders and employees of the Klima Consulting company, that aims at reducing the climate impact of aviation, among other objectives. CS and NB declare that they have no competing interests.

Acknowledgements. The authors thank Étienne Vignon for reviewing and commenting on a preliminary version of the manuscript. This research has been supported by the French Ministère de la Transition Écologique et Solidaire under the Climaviation project (grant DGAC N2021-39), with support from France's Plan National de Relance et de Résilience (PNRR) and the European Union's NextGenerationEU.
525 This study benefited from the IPSL mesocenter ESPRI facility which is supported by CNRS, Sorbonne Université, Labex L-IPSL, CNES and École Polytechnique.



References

Akhtar Martínez, C. and Jarrett, J.: Comparing two contrail models under certain and uncertain inputs, in: AIAA SCITECH 2024 Forum, AIAA SciTech Forum, American Institute of Aeronautics and Astronautics, <https://doi.org/10.2514/6.2024-1023>, 2024.

530 Akhtar Martínez, C., Eastham, S. D., and Jarrett, J. P.: Zero-dimensional contrail models could underpredict lifetime optical depth, Atmospheric Chemistry and Physics, 25, 12 875–12 891, <https://doi.org/10.5194/acp-25-12875-2025>, 2025.

Bickel, M., Ponater, M., Burkhardt, U., Righi, M., Hendricks, J., and Jöckel, P.: Contrail cirrus climate impact: From radiative forcing to surface temperature change, Journal of Climate, 38, 1895–1912, <https://doi.org/10.1175/JCLI-D-24-0245.1>, 2025.

Borella, A., Boucher, O., Shine, K. P., Stettler, M., Tanaka, K., Teoh, R., and Bellouin, N.: The importance of an informed choice of 535 CO₂-equivalence metrics for contrail avoidance, Atmospheric Chemistry and Physics, 24, 9401–9417, <https://doi.org/10.5194/acp-24-9401-2024>, 2024.

Boucher, O., Bellouin, N., Clark, H., Gryspeerdt, E., and Karadayi, J.: Comparison of actual and time-optimized flight trajectories in the context of the In-service Aircraft for a Global Observing System (IAGOS) programme, Aerospace, 10, 744, <https://doi.org/10.3390/aerospace10090744>, 2023.

540 Boulanger, D., Blot, R., Bundke, U., Gerbig, C., Hermann, M., Nédélec, P., Rohs, S., and Ziereis, H.: IAGOS final quality controlled Observational Data L2 – Time series, Aeris [Dataset], <https://doi.org/10.25326/06> (last access: 16 November 2023), 2018.

Brasseur, G. P., Gupta, M., Anderson, B. E., Balasubramanian, S., Barrett, S., Duda, D., Fleming, G., Forster, P. M., Fuglestvedt, J., Gettelman, A., Halthore, R. N., Jacob, S. D., Jacobson, M. Z., Khodayari, A., Liou, K.-N., Lund, M. T., Miake-Lye, R. C., Minnis, P., Olsen, S., Penner, J. E., Prinn, R., Schumann, U., Selkirk, H. B., Sokolov, A., Unger, N., Wolfe, P., Wong, H.-W., Wuebbles, D. W., Yi, B., Yang, 545 P., and Zhou, C.: Impact of aviation on climate: FAA's Aviation Climate Change Research Initiative (ACCR) Phase II, Bulletin of the American Meteorological Society, 97, 561–583, <https://doi.org/10.1175/BAMS-D-13-00089.1>, 2016.

Burkhardt, U. and Kärcher, B.: Global radiative forcing from contrail cirrus, Nature Climate Change, 1, 54–58, <https://doi.org/10.1038/nclimate1068>, 2011.

Burkhardt, U., Bock, L., and Bier, A.: Mitigating the contrail cirrus climate impact by reducing aircraft soot number emissions, npj Climate 550 and Atmospheric Science, 1, 1–7, <https://doi.org/10.1038/s41612-018-0046-4>, 2018.

Castino, F., Yin, F., Grewe, V., Yamashita, H., Matthes, S., Dietmüller, S., Baumann, S., Soler, M., Simorgh, A., Mendiguchia Meuser, M., Linke, F., and Lührs, B.: Decision-making strategies implemented in SolFinder 1.0 to identify eco-efficient aircraft trajectories: Application study in AirTraf 3.0, Geoscientific Model Development, 17, 4031–4052, <https://doi.org/10.5194/gmd-17-4031-2024>, 2024.

Dean, T. R., Abbott, T. H., Engberg, Z., Masson, N., Teoh, R., Itcovitz, J. P., Stettler, M. E. J., and Shapiro, M. L.: Impact of forecast stability 555 on navigational contrail avoidance, Environmental Research: Infrastructure and Sustainability, 5, 045 008, <https://doi.org/10.1088/2634-4505/ae1da5>, 2025.

DuBois, D. and Paynter, G. C.: “Fuel Flow Method 2” for estimating aircraft emissions, SAE Transactions, 115, 1–14, <https://doi.org/10.4271/2006-01-1987>, 2006.

EASA: Updated analysis of the non-CO₂ climate impacts of aviation and potential policy measures pursuant to the EU Emissions 560 Trading System Directive Article 30(4), European Union Aviation Safety Agency, <https://www.easa.europa.eu/en/document-library/research-reports/report-commission-european-parliament-and-council> (last access: 17 October 2023), 192 pp, 2020.

EASA: ICAO aircraft engine emissions databank [Dataset], European Union Aviation Safety Agency, <https://www.easa.europa.eu/domains/environment/icao-aircraft-engine-emissions-databank> (last access: 26 August 2025), 2025.



ECMWF: IFS Documentation CY49R1 - Part V: Ensemble Prediction System, in: IFS Documentation CY49R1, ECMWF,
565 https://doi.org/10.21957/956d60ad81, 2024a.

ECMWF: IFS Documentation CY49R1 - Part IV: Physical Processes, in: IFS Documentation CY49R1, ECMWF,
https://doi.org/10.21957/c731ee1102, 2024b.

Engberg, Z., Teoh, R., Abbott, T., Dean, T., Stettler, M. E. J., and Shapiro, M. L.: Forecasting contrail climate forcing for flight planning
and air traffic management applications: the CocipGrid model in pycontrails 0.51.0, Geoscientific Model Development, 18, 253–286,
570 https://doi.org/10.5194/gmd-18-253-2025, 2025.

EUROCONTROL: User manual for the Base of Aircraft Data (BADA) Revision 3.15. EEC Technical/Scientific Report No. 19/03/18-45,
EUROCONTROL Experimental Centre (EEC), <https://www.eurocontrol.int/model/bada> (last access: 26 August 2025), 2019.

FlightRadar24: Flight database [Dataset], <https://www.flightradar24.com> (last access: 26 August 2025), 2022.

Forster, C., Stohl, A., James, P., and Thouret, V.: The residence times of aircraft emissions in the stratosphere using a mean emission inventory
575 and emissions along actual flight tracks, Journal of Geophysical Research: Atmospheres, 108, <https://doi.org/10.1029/2002JD002515>, 2003.

Fritz, T. M., Eastham, S. D., Speth, R. L., and Barrett, S. R. H.: The role of plume-scale processes in long-term impacts of aircraft emissions,
Atmospheric Chemistry and Physics, 20, 5697–5727, <https://doi.org/10.5194/acp-20-5697-2020>, 2020.

Frömming, C., Grewe, V., Brinkop, S., Jöckel, P., Haslerud, A. S., Rosanka, S., van Manen, J., and Matthes, S.: Influence of weather situation
580 on non-CO₂ aviation climate effects: The REACT4C climate change functions, Atmospheric Chemistry and Physics, 21, 9151–9172,
<https://doi.org/10.5194/acp-21-9151-2021>, 2021.

Gasser, T., Ciais, P., Boucher, O., Quilcaillie, Y., Tortora, M., Bopp, L., and Hauglustaine, D.: The compact Earth system model OSCAR v2.2:
description and first results, Geoscientific Model Development, 10, 271–319, <https://doi.org/10.5194/gmd-10-271-2017>, 2017.

Gierens, K., Spichtinger, P., and Schumann, U.: Ice supersaturation, in: Atmospheric Physics: Background – Methods – Trends,
585 edited by Schumann, U., Research Topics in Aerospace, pp. 135–150, Springer, Berlin, Heidelberg, ISBN 978-3-642-30183-4,
https://doi.org/10.1007/978-3-642-30183-4_9, 2012.

Gierens, K., Matthes, S., and Rohs, S.: How well can persistent contrails be predicted?, Aerospace, 7, 169,
<https://doi.org/10.3390/aerospace7120169>, 2020.

Grewe, V. and Stenke, A.: AirClim: An efficient tool for climate evaluation of aircraft technology, Atmospheric Chemistry and Physics, 8,
590 4621–4639, <https://doi.org/10.5194/acp-8-4621-2008>, 2008.

Grewe, V., Frömming, C., Matthes, S., Brinkop, S., Ponater, M., Dietmüller, S., Jöckel, P., Garny, H., Tsati, E., Dahlmann, K., Søvde,
O. A., Fuglestvedt, J., Berntsen, T. K., Shine, K. P., Irvine, E. A., Champougny, T., and Hullah, P.: Aircraft routing with mini-
595 mal climate impact: the REACT4C climate cost function modelling approach (V1.0), Geoscientific Model Development, 7, 175–201,
<https://doi.org/10.5194/gmd-7-175-2014>, 2014.

Grewe, V., Matthes, S., Frömming, C., Brinkop, S., Jöckel, P., Gierens, K., Champougny, T., Fuglestvedt, J., Haslerud, A., Irvine, E., and
Shine, K.: Feasibility of climate-optimized air traffic routing for trans-Atlantic flights, Environmental Research Letters, 12, 034003,
600 <https://doi.org/10.1088/1748-9326/aa5ba0>, 2017.

Hanst, M., Köhler, C. G., Seifert, A., and Schlemmer, L.: Predicting ice supersaturation for contrail avoidance: ensemble forecasting us-
ing ICON with two-moment ice microphysics, Atmospheric Chemistry and Physics, 25, 17 253–17 274, <https://doi.org/10.5194/acp-25-17253-2025>, 2025.



Hildebrandt, K. G., Castino, F., Meijer, V., and Yin, F.: Variability of ice supersaturated regions at flight altitudes: evaluation of ERA5 reanalysis using IAGOS in situ measurements, *EGU*sphere, pp. 1–35, <https://doi.org/10.5194/egusphere-2025-3048>, 2025.

Hofer, S., Gierens, K., and Rohs, S.: How well can persistent contrails be predicted? An update, *Atmospheric Chemistry and Physics*, 24, 7911–7925, <https://doi.org/10.5194/acp-24-7911-2024>, 2024.

605 ICCT: CO₂ emissions from commercial aviation 2018, by: Graver, B., Zhang, K., and Rutherford, D., International Council on Clean Transportation, https://theicct.org/wp-content/uploads/2021/06/ICCT_CO2-commercl-aviation-2018_20190918.pdf (last access: 17 October 2023), 2018.

Irvine, E. A., Hoskins, B. J., and Shine, K. P.: A simple framework for assessing the trade-off between the climate impact of aviation carbon dioxide emissions and contrails for a single flight, *Environmental Research Letters*, 9, 064021, <https://doi.org/10.1088/1748-9326/9/6/064021>, 2014.

610 Jafarimoghaddam, A. and Soler, M.: A multi-physics Eulerian framework for long-term contrail evolution, *EGU*sphere, pp. 1–46, <https://doi.org/10.5194/egusphere-2025-4155>, 2025.

Jaramillo, P., Kahn Ribeiro, S., Newman, P., Dhar, S., Diemuodeke, O. E., Kajino, T., Lee, D. S., Nugroho, S., Ou, X., Hammer Strømman, A., and Whitehead, J.: Transport, in: *Climate Change 2022: Mitigation of Climate Change. Contribution of Working Group III to the Sixth Assessment Report of the Intergovernmental Panel on Climate Change*, edited by Shukla, P. R., Skea, J., Slade, R., Al Khourdajie, A., van Diemen, R., McCollum, D., Pathak, M., Some, S., Vyas, P., Fradera, R., Belkacemi, M., Hasija, A., Lisboa, G., Luz, S., and Malley, J., pp. 1049–1160, Cambridge University Press, Cambridge, United Kingdom and New York, NY, USA, ISBN 978-1-009-15792-6, <https://doi.org/10.1017/9781009157926.012>, 2023.

Johansson, D. J. A., Azar, C., Pettersson, S., Sterner, T., Stettler, M. E. J., and Teoh, R.: The social costs of aviation CO₂ and contrail cirrus, *Nature Communications*, 16, 8558, <https://doi.org/10.1038/s41467-025-64355-5>, 2025.

Klöwer, M., Allen, M. R., Lee, D. S., Proud, S. R., Gallagher, L., and Skowron, A.: Quantifying aviation's contribution to global warming, *Environmental Research Letters*, 16, 104027, <https://doi.org/10.1088/1748-9326/ac286e>, 2021.

Kärcher, B.: Formation and radiative forcing of contrail cirrus, *Nature Communications*, 9, 1824, <https://doi.org/10.1038/s41467-018-04068-0>, 2018.

625 Köhler, M. O., Rädel, G., Shine, K. P., Rogers, H. L., and Pyle, J. A.: Latitudinal variation of the effect of aviation NO_x emissions on atmospheric ozone and methane and related climate metrics, *Atmospheric Environment*, 64, 1–9, <https://doi.org/10.1016/j.atmosenv.2012.09.013>, 2013.

Lee, D., Fahey, D., Skowron, A., Allen, M., Burkhardt, U., Chen, Q., Doherty, S., Freeman, S., Forster, P., Fuglestvedt, J., Gettelman, A., De León, R., Lim, L., Lund, M., Millar, R., Owen, B., Penner, J., Pitari, G., Prather, M., Sausen, R., and Wilcox, L.: 630 The contribution of global aviation to anthropogenic climate forcing for 2000 to 2018, *Atmospheric Environment*, 244, 117834, <https://doi.org/10.1016/j.atmosenv.2020.117834>, 2021.

Lee, D. S., R. Allen, M., Cumpsty, N., Owen, B., P. Shine, K., and Skowron, A.: Uncertainties in mitigating aviation non-CO₂ emissions for climate and air quality using hydrocarbon fuels, *Environmental Science: Atmospheres*, <https://doi.org/10.1039/D3EA00091E>, 2023.

Mannstein, H., Spichtinger, P., and Gierens, K.: A note on how to avoid contrail cirrus, *Transportation Research Part D: Transport and Environment*, 10, 421–426, <https://doi.org/10.1016/j.trd.2005.04.012>, 2005.

635 Martín Frías, A., Shapiro, M. L., Engberg, Z., Zopp, R., Soler, M., and Stettler, M. E. J.: Feasibility of contrail avoidance in a commercial flight planning system: an operational analysis, *Environmental Research: Infrastructure and Sustainability*, 4, 015013, <https://doi.org/10.1088/2634-4505/ad310c>, 2024.



Matthes, S., Lührs, B., Dahlmann, K., Grewe, V., Linke, F., Yin, F., Klingaman, E., and Shine, K. P.: Climate-optimized trajectories and
640 robust mitigation potential: Flying ATM4E, *Aerospace*, 7, 156, <https://doi.org/10.3390/aerospace7110156>, 2020.

Megill, L., Deck, K., and Grewe, V.: Alternative climate metrics to the Global Warming Potential are more suitable for assessing aviation
non-CO₂ effects, *Communications Earth & Environment*, 5, 1–9, <https://doi.org/10.1038/s43247-024-01423-6>, 2024.

Molloy, J., Teoh, R., Harty, S., Koudis, G., Schumann, U., Poll, I., and Stettler, M. E. J.: Design principles for a contrail-minimizing trial in
the North Atlantic, *Aerospace*, 9, 375, <https://doi.org/10.3390/aerospace9070375>, 2022.

645 Märkl, R. S., Voigt, C., Sauer, D., Dischl, R. K., Kaufmann, S., Harlaß, T., Hahn, V., Roiger, A., Weiß-Rehm, C., Burkhardt, U., Schumann,
U., Marsing, A., Scheibe, M., Dörnbrack, A., Renard, C., Gauthier, M., Swann, P., Madden, P., Luff, D., Sallinen, R., Schripp, T., and
Le Clercq, P.: Powering aircraft with 100% sustainable aviation fuel reduces ice crystals in contrails, *Atmospheric Chemistry and Physics*,
24, 3813–3837, <https://doi.org/10.5194/acp-24-3813-2024>, 2024.

Niklaß, M., Linke, F., Dahlmann, K., Grewe, V., Matthes, S., Plohr, M., Maertens, S., Wozny, F., and Scheelhaase, J.: Decision parameters
650 of an MRV scheme for integrating non-CO₂ aviation effects into EU ETS, https://www.umweltbundesamt.de/sites/default/files/medien/11850/publikationen/30_2024_cc_decision_parameters.pdf (last access: 26 August 2025), 2024.

Niklaß, M., Lührs, B., Grewe, V., Dahlmann, K., Luchkova, T., Linke, F., and Gollnick, V.: Potential to reduce the climate impact of aviation
by climate restricted airspaces, *Transport Policy*, 83, 102–110, <https://doi.org/10.1016/j.tranpol.2016.12.010>, 2019.

Nuic, A., Poles, D., and Mouillet, V.: BADA: An advanced aircraft performance model for present and future ATM systems, *International
655 Journal of Adaptive Control and Signal Processing*, 24, 850–866, <https://doi.org/10.1002/acs.1176>, 2010.

Petzold, A., Thouret, V., Gerbig, C., Zahn, A., Brenninkmeijer, C. A. M., Gallagher, M., Hermann, M., Pontaud, M., Ziereis, H., Boulanger,
D., Marshall, J., Nédélec, P., Smit, H. G. J., Friess, U., Flaud, J.-M., Wahner, A., Cammas, J.-P., and Volz-Thomas, A.: Global-scale
atmosphere monitoring by in-service aircraft – current achievements and future prospects of the European Research Infrastructure IAGOS,
Tellus B: Chemical and Physical Meteorology, 67, 28 452, <https://doi.org/10.3402/tellusb.v67.28452>, 2015.

660 Platt, J. C., Shapiro, M. L., Engberg, Z., McCloskey, K., Geraedts, S., Sankar, T., Stettler, M. E. J., Teoh, R., Schumann, U., Rohs, S.,
Brand, E., and Arsdale, C. V.: The effect of uncertainty in humidity and model parameters on the prediction of contrail energy forcing,
Environmental Research Communications, 6, 095 015, <https://doi.org/10.1088/2515-7620/ad6ee5>, 2024.

Poles, D., Nuic, A., and Mouillet, V.: Advanced aircraft performance modeling for ATM: Analysis of BADA model capabilities, in: 29th
Digital Avionics Systems Conference, pp. 1.D.1–1–1.D.1–14, <https://doi.org/10.1109/DASC.2010.5655518>, 2010.

665 Ponater, M., Marquart, S., Sausen, R., and Schumann, U.: On contrail climate sensitivity, *Geophysical Research Letters*, 32,
<https://doi.org/10.1029/2005GL022580>, 2005.

Prather, M. J., Gettelman, A., and Penner, J. E.: Trade-offs in aviation impacts on climate favour non-CO₂ mitigation, *Nature*, pp. 1–6,
<https://doi.org/10.1038/s41586-025-09198-2>, 2025.

Quante, G., Voß, S., Bullerdiek, N., Voigt, C., and Kaltschmitt, M.: Hydroprocessing of fossil fuel-based aviation kerosene – Technology
670 options and climate impact mitigation potentials, *Atmospheric Environment: X*, 22, 100 259, <https://doi.org/10.1016/j.aeaoa.2024.100259>,
2024.

Rao, P., Yin, F., Grewe, V., Yamashita, H., Jöckel, P., Matthes, S., Mertens, M., and Frömming, C.: Case study for testing
the validity of NO_x-ozone algorithmic climate change functions for optimising flight trajectories, *Aerospace*, 9, 231,
<https://doi.org/10.3390/aerospace9050231>, 2022.

675 Rap, A., Forster, P. M., Haywood, J. M., Jones, A., and Boucher, O.: Estimating the climate impact of linear contrails using the UK Met
Office climate model, *Geophysical Research Letters*, 37, <https://doi.org/10.1029/2010GL045161>, 2010.



Reutter, P., Neis, P., Rohs, S., and Sauvage, B.: Ice supersaturated regions: properties and validation of ERA-Interim reanalysis with IAGOS in situ water vapour measurements, *Atmospheric Chemistry and Physics*, 20, 787–804, <https://doi.org/10.5194/acp-20-787-2020>, 2020.

Rosenow, J., Fricke, H., Luchkova, T., and Schultz, M.: Minimizing contrail formation by rerouting around dynamic ice-supersaturated regions, *Aeronautics and Aerospace Open Access Journal*, 2, <https://doi.org/10.15406/aaoj.2018.02.00039>, 2018.

Sausen, R., Hofer, S., Gierens, K., Bugliaro, L., Ehrmanntraut, R., Sitova, I., Walczak, K., Burridge-Diesing, A., Bowman, M., and Miller, N.: Can we successfully avoid persistent contrails by small altitude adjustments of flights in the real world?, *Meteorologische Zeitschrift*, 33, 83–98, <https://doi.org/10.1127/metz/2023/1157>, 2024.

Schumann, U.: On conditions for contrail formation from aircraft exhausts, *Meteorologische Zeitschrift*, pp. 4–23, <https://doi.org/10.1127/metz/5/1996/4>, 1996.

Schumann, U.: A contrail cirrus prediction model, *Geoscientific Model Development*, 5, 543–580, <https://doi.org/10.5194/gmd-5-543-2012>, 2012.

Schumann, U., Mayer, B., Graf, K., and Mannstein, H.: A parametric radiative forcing model for contrail cirrus, *Journal of Applied Meteorology and Climatology*, 51, 1391–1406, <https://doi.org/10.1175/JAMC-D-11-0242.1>, 2012.

Shapiro, M., Engberg, Z., Teoh, R., Stettler, M., Dean, T., and Abbott, T.: pycontrails: Python library for modeling aviation climate impacts, <https://doi.org/10.5281/zenodo.15426480>, 2025.

Simorgh, A. and Soler, M.: Climate-optimized flight planning can effectively reduce the environmental footprint of aviation in Europe at low operational costs, *Communications Earth & Environment*, 6, 1–13, <https://doi.org/10.1038/s43247-025-02031-8>, 2025.

Simorgh, A., Soler, M., González-Arribas, D., Linke, F., Lührs, B., Meuser, M. M., Dietmüller, S., Matthes, S., Yamashita, H., Yin, F., Castino, F., Grewe, V., and Baumann, S.: Robust 4D climate-optimal flight planning in structured airspace using parallelized simulation on GPUs: ROOST V1.0, *Geoscientific Model Development*, 16, 3723–3748, <https://doi.org/10.5194/gmd-16-3723-2023>, 2023.

Simorgh, A., Soler, M., Castino, F., Yin, F., and Cerezo-Magaña, M.: Concept of robust climate-friendly flight planning under multiple climate impact estimates, *Transportation Research Part D: Transport and Environment*, 131, 104215, <https://doi.org/10.1016/j.trd.2024.104215>, 2024a.

Simorgh, A., Soler, M., Dietmüller, S., Matthes, S., Yamashita, H., Castino, F., and Yin, F.: Robust 4D climate-optimal aircraft trajectory planning under weather-induced uncertainties: Free-routing airspace, *Transportation Research Part D: Transport and Environment*, 131, 104196, <https://doi.org/10.1016/j.trd.2024.104196>, 2024b.

Smith, J., Grobler, C., Hodgson, P. J., Mukhopadhyaya, J., Shapiro, M., Mirolo, M., Stettler, M., Eastham, S., and Barrett, S.: The climate opportunities and risks of contrail avoidance, <https://doi.org/10.21203/rs.3.rs-6925120/v1>, 2025.

Soci, C., Hersbach, H., Simmons, A., Poli, P., Bell, B., Berrisford, P., Horányi, A., Muñoz-Sabater, J., Nicolas, J., Radu, R., Schepers, D., Villaume, S., Haimberger, L., Woollen, J., Buontempo, C., and Thépaut, J.-N.: The ERA5 global reanalysis from 1940 to 2022, *Quarterly Journal of the Royal Meteorological Society*, 150, 4014–4048, <https://doi.org/10.1002/qj.4803>, 2024.

Sonabend-W, A., Elkin, C., Dean, T., Dudley, J., Ali, N., Blickstein, J., Brand, E., Broshears, B., Chen, S., Engberg, Z., Galyen, M., Geraedts, S., Goyal, N., Grenham, R., Hager, U., Hecker, D., Jany, M., McCloskey, K., Ng, J., Norris, B., Opel, F., Rothenberg, J., Sankar, T., Sanekommu, D., Sarna, A., Schütt, O., Shapiro, M., Soh, R., Van Arsdale, C., and Platt, J. C.: Feasibility test of per-flight contrail avoidance in commercial aviation, *Communications Engineering*, 3, 1–7, <https://doi.org/10.1038/s44172-024-00329-7>, 2024.

Teoh, R., Schumann, U., Majumdar, A., and Stettler, M. E. J.: Mitigating the climate forcing of aircraft contrails by small-scale diversions and technology adoption, *Environmental Science & Technology*, 54, 2941–2950, <https://doi.org/10.1021/acs.est.9b05608>, 2020.



715 Teoh, R., Schumann, U., Gryspeerdt, E., Shapiro, M., Molloy, J., Koudis, G., Voigt, C., and Stettler, M. E. J.: Aviation contrail climate effects in the North Atlantic from 2016 to 2021, *Atmospheric Chemistry and Physics*, 22, 10 919–10 935, <https://doi.org/10.5194/acp-22-10919-2022>, 2022.

Teoh, R., Engberg, Z., Schumann, U., Voigt, C., Shapiro, M., Rohs, S., and Stettler, M. E. J.: Global aviation contrail climate effects from 2019 to 2021, *Atmospheric Chemistry and Physics*, 24, 6071–6093, <https://doi.org/10.5194/acp-24-6071-2024>, 2024a.

720 Teoh, R., Engberg, Z., Shapiro, M., Dray, L., and Stettler, M. E. J.: The high-resolution global aviation emissions inventory based on ADS-B (GAIA) for 2019–2021, *Atmospheric Chemistry and Physics*, 24, 725–744, <https://doi.org/10.5194/acp-24-725-2024>, 2024b.

725 UNFCCC: Decision 4/CP.1 Methodological issues, United Nations Framework Convention on Climate Change, <https://unfccc.int/decisions?f%5B0%5D=session%3A3851> (last access: 17 October 2023), 1995.

UNFCCC: Report of the Conference of the Parties serving as the meeting of the Parties to the Paris Agreement on the third part of its first session, held in Katowice from 2 to 15 December 2018, Addendum 2. Part two: Action taken by the Conference of the Parties serving as the meeting of the Parties to the Paris Agreement (FCCC/PA/CMA/2018/3/Add.2 2019), United Nations Framework Convention on Climate Change, https://unfccc.int/sites/default/files/resource/cma2018_3_add2_new_advance.pdf (last access: 12 December 2023), 2019.

730 van Manen, J. and Grewe, V.: Algorithmic climate change functions for the use in eco-efficient flight planning, *Transportation Research Part D: Transport and Environment*, 67, 388–405, <https://doi.org/10.1016/j.trd.2018.12.016>, 2019.

735 Voigt, C., Kleine, J., Sauer, D., Moore, R. H., Bräuer, T., Le Clercq, P., Kaufmann, S., Scheibe, M., Jurkat-Witschas, T., Aigner, M., Bauder, U., Boose, Y., Borrman, S., Crosbie, E., Diskin, G. S., DiGangi, J., Hahn, V., Heckl, C., Huber, F., Nowak, J. B., Rapp, M., Rauch, B., Robinson, C., Schripp, T., Shook, M., Winstead, E., Ziembka, L., Schlager, H., and Anderson, B. E.: Cleaner burning aviation fuels can reduce contrail cloudiness, *Communications Earth & Environment*, 2, 114, <https://doi.org/10.1038/s43247-021-00174-y>, 2021.

740 von Bonhorst, G., Maizet, M., and Gierens, K.: On contrail prediction under realistic weather forecast uncertainty using the example of WAWFOR data, *Meteorologische Zeitschrift*, <https://doi.org/10.1127/metz/1251>, 2025.

745 Wang, Z., Bugliaro, L., Gierens, K., Hegglin, M. I., Rohs, S., Petzold, A., Kaufmann, S., and Voigt, C.: Machine learning for improvement of upper-tropospheric relative humidity in ERA5 weather model data, *Atmospheric Chemistry and Physics*, 25, 2845–2861, <https://doi.org/10.5194/acp-25-2845-2025>, 2025.

750 Wilkerson, J. T., Jacobson, M. Z., Malwitz, A., Balasubramanian, S., Wayson, R., Fleming, G., Naiman, A. D., and Lele, S. K.: Analysis of emission data from global commercial aviation: 2004 and 2006, *Atmospheric Chemistry and Physics*, 10, 6391–6408, <https://doi.org/10.5194/acp-10-6391-2010>, 2010.

Wolf, K., Bellouin, N., Boucher, O., Rohs, S., and Li, Y.: Correction of ERA5 temperature and relative humidity biases by bivariate quantile mapping for contrail formation analysis, *Atmospheric Chemistry and Physics*, 25, 157–181, <https://doi.org/10.5194/acp-25-157-2025>, 2025.

745 Yamashita, H., Yin, F., Grewe, V., Jöckel, P., Matthes, S., Kern, B., Dahlmann, K., and Frömming, C.: Newly developed aircraft routing options for air traffic simulation in the chemistry–climate model EMAC 2.53: AirTraf 2.0, *Geoscientific Model Development*, 13, 4869–4890, <https://doi.org/10.5194/gmd-13-4869-2020>, 2020.

750 Yamashita, H., Yin, F., Grewe, V., Jöckel, P., Matthes, S., Kern, B., Dahlmann, K., and Frömming, C.: Analysis of aircraft routing strategies for North Atlantic flights by using AirTraf 2.0, *Aerospace*, 8, 33, <https://doi.org/10.3390/aerospace8020033>, 2021.

Yin, F., Grewe, V., Castino, F., Rao, P., Matthes, S., Dahlmann, K., Dietmüller, S., Frömming, C., Yamashita, H., Peter, P., Klingaman, E., Shine, K. P., Lührs, B., and Linke, F.: Predicting the climate impact of aviation for en-route emissions: the algorithmic climate change



function submodel ACCF 1.0 of EMAC 2.53, *Geoscientific Model Development*, 16, 3313–3334, <https://doi.org/10.5194/gmd-16-3313-2023>, 2023.

Zengerling, Z. L., Linke, F., Weder, C. M., Dietmüller, S., Matthes, S., and Peter, P.: Flying low and slow: Application of algorithmic climate change functions to assess the climate mitigation potential of reduced cruise altitudes and speeds on different days, *Meteorologische Zeitschrift*, pp. 67–81, <https://doi.org/10.1127/metz/2023/1194>, 2024.

755